AN INVESTIGATION OF THE SELF-PRESSURE BROADENING OF THE Ne λ6074.3 A^{o} LINE PROFILE BY ZEEMAN SCANNING

by

JOHN C. BURNETT

B.Sc., University of British Columbia, 1959

A THESIS SUBMITTED IN PARTIAL FULFILMENT OF THE REQUIREMENTS FOR THE DEGREE OF

MASTER OF SCIENCE

in the Department of

PHYSICS

We accept this thesis as conforming to the required standard:

THE UNIVERSITY OF BRITISH COLUMBIA

November, 1969

In presenting this thesis in partial fulfilment of the requirements for an advanced degree at the University of British Columbia, I agree that the Library shall make it freely available for reference and Study. I further agree that permission for extensive copying of this thesis for scholarly purposes may be granted by the Head of my Department or by his representatives. It is understood that copying or publication of this thesis for financial gain shall not be allowed without my written permission.

John C. Burnett)

Department of Physics

The University of British Columbia
Vancouver 8, Canada

Date 10 Nov, 1969

Abstract

The shape of the Ne λ6074.3 A^{o} absorption line profile has been investigated using the Zeeman scanning technique.

Neon glow discharges at three pressures, 2 Torr, 50 Torr, and 100 Torr, were used as absorbers while a 2 Torr Geissler tube was used as the source. The self-pressure broadening of the observed line was clearly observed and the rate of broadening compares well with theoretical estimates made from the impact theory with a van der Waals interaction assumed.

No shift was detected, in contradiction to the theory. This lack of shift, and the rate of pressure broadening observed, were in agreement with the results of Smith (14) regarding the shift and broadening of the Ca λ6573 A^{o} line by neon.

TABLE OF CONTENTS

LIST OF FIGURES

LIST OF REFERENCED EQUATIONS

Acknowledgements

I wish to express my appreciation to Dr. R. Nodwell for his encouragement and support, both of my graduate work in general and this experiment. I also wish to thank Dr. J. Meyer for his guidance and advice in the preparation of this thesis.

Additional thanks are due to:

- Mr. Barry Stansfield for his initial work setting up the Zeeman scanning system and demonstrating its feasibility.
- Mr. Barry Stansfield and Dr. W. Seka for much helpful discussion and advice.
- Mr. J. Lees for his expert construction and filling of the source and absorber tubes.

Finally I wish to express my gratitude to my wife, Sylvia, for her continuing patience and support.

CHAPTER I

INTRODUCTION

Spectral lines, both in emission and absorption, are characterized by their shape, frequency, and intensity or strength. The shape of a spectral line is primarily determined by the physical environment of its source, in particular the temperature, neutral particle density, electron density, and electric or magnetic fields present. For most high temperature plasmas in the absence of strong electromagnetic fields the shape of the line is determined by the temperature and electron density. At lower temperatures it is the temperature and neutral particle density which are usually most significant.

Geissler tube and glow discharge plasmas, which belong to the latter class of lower temperature plasmas, are frequently employed in spectroscopic work as sources or absorbers of spectral lines. For example in two recent experiments at the University of British Columbia the absorption in glow discharges of light emitted by Geissler tubes has been used to measure relative transition probabilities in neon. One experiment compared the absorption strengths of various spectral lines(1) while the second utilized Faraday rotation in a glow discharge tube(2). In both experiments it was assumed that the absorption and emission line shapes were Gaussian, due to thermal Doppler broadening alone. Appreciable

departure from the Gaussian shapes assumed could affect the validity of these results.

Estimates of pressure broadening, made according to the impact theory under the assumption of a van der Waals interaction, indicate that under glow discharge conditions there may indeed be sufficient pressure broadening to alter the line shapes significantly. In addition this theory predicts a slight, pressure dependent, decrease in the frequency of the spectral line.

It was thus desirable to examine at least one such neon glow discharge line not only to check the validity of the assumption of Gaussian line shapes but also to test the theoretical predictions. However the spectral lines in glow discharge and Geissler tube plasmas are too narrow to be conveniently studied by conventional spectrographic techniques unless equipment of very high resolution ($\frac{\Delta\lambda}{\lambda} \gtrsim 10^6$) is employed.

It had been demonstrated by Stansfield (3) that with the Zeeman scanning technique of Bitter et al (4) it should be possible to discern the exact shape of such narrow spectral lines. With this technique a single σ-component of a normal Zeeman triplet is isolated and employed as a variable frequency source. It is passed through an absorber to scan the absorption line under examination. The fractional transmission is obtained for a range of source frequencies sufficient to span the absorption line. The resultant transmission curves generally reflect the shapes of both the

source and the absorber and are sensitive to variations in either. By comparing these results to the predictions of a simple model the line shapes of source and absorber may be extracted.

As employed in this experiment the technique seemed capable of detecting changes in the width of an absorption line as small as 2 mA^{o} (which for the line studied corresponds to 10% or less of the half width). It also seemed capable of quite accurate determination of the line shape. Because the Zeeman scanning apparatus is composed of equipment usually available in a laboratory or else obtainable at low cost, the technique seemed attractive as a simple, economic means of studying the shape of a narrow line from a neon glow discharge.

CHAPTER II

THEORY

A. Spectral Line Absorption and Transmission Curves

As radiation passes through an element of absorbing medium the fraction of this radiation absorbed is directly proportional to the absorbing 'strength' of the medium and the length of the absorber traversed.

$$\frac{dI(\nu)}{I(\nu)} = - k(\nu)dx \qquad \text{I}$$

$I(\nu)$ is the intensity of the radiation at frequency ν.

$k(\nu)$ is the absorption constant ('strength' of the absorber) at frequency ν.

dx is the elemental length of absorber traversed.

Integrating for a homogeneous absorber of length ℓ and denoting the incident intensity by $I_i(\nu)$ and the transmitted intensity by $I_\ell(\nu)$:

$$I_\ell(\nu) = I_i(\nu)\exp\{ - k(\nu)\ell \} \qquad \text{II}$$

The absorber will itself emit light at frequency ν. This light will have an intensity comparable to $I_i(\nu)$. However the source is intensity modulated and a lock-in amplifier is employed to determine the transmitted intensity. The unmodulated light emitted by the absorber is rejected as noise by the phase sensitive detection system. Since the lock-in amplifier

used improved the signal-to-noise ratio by a factor of 100 or more, the light emitted by the absorber may be omitted from consideration. Hence Equation II gives exactly the intensity emergent from an absorber of length ℓ .

In the region of an absorption line $k(\nu)$ will have a frequency dependence peaking at the line centre ν_0 as indicated below.

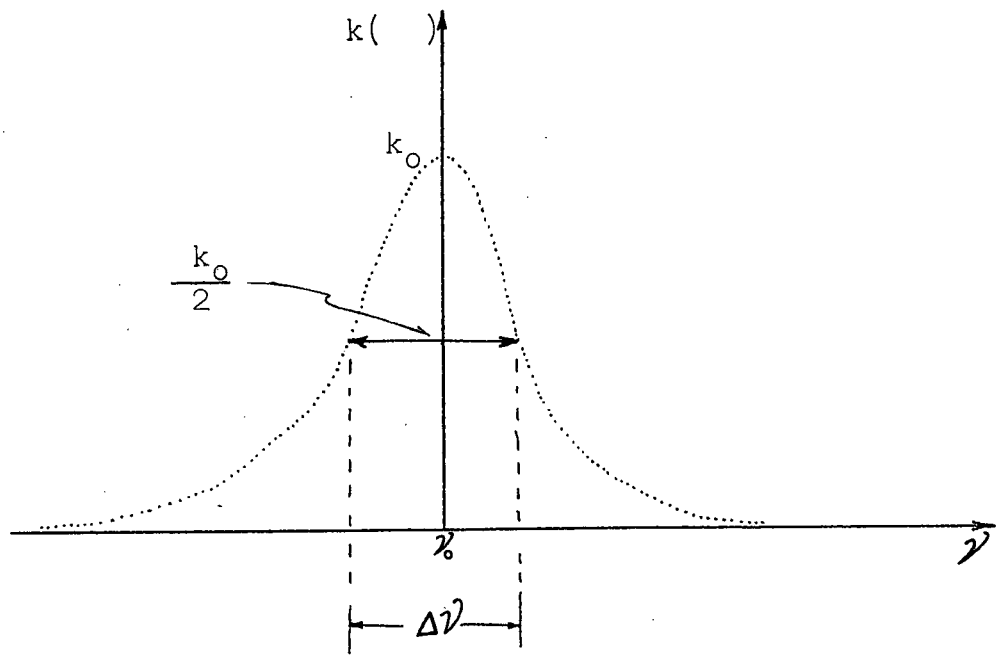

A useful measure of the width of an absorption line is the half width $\Delta\nu$ which is here defined as the full width at the half-maximum of $k(\nu)$ - see above.

If a band of radiation with frequency mean ν_s characterized by the shape $I_i(\nu - \nu_s)$ is passed through a length ℓ of absorber specified by $k(\nu) \equiv k(\nu - \nu_0)$ where ν_0 is the central frequency of the absorber, then the resultant intensity at frequency ν' is:

$$I_f(\nu') = I_i(\nu' - \nu_s)\exp\{-k(\nu' - \nu_0)\ell\} \qquad \text{III}$$

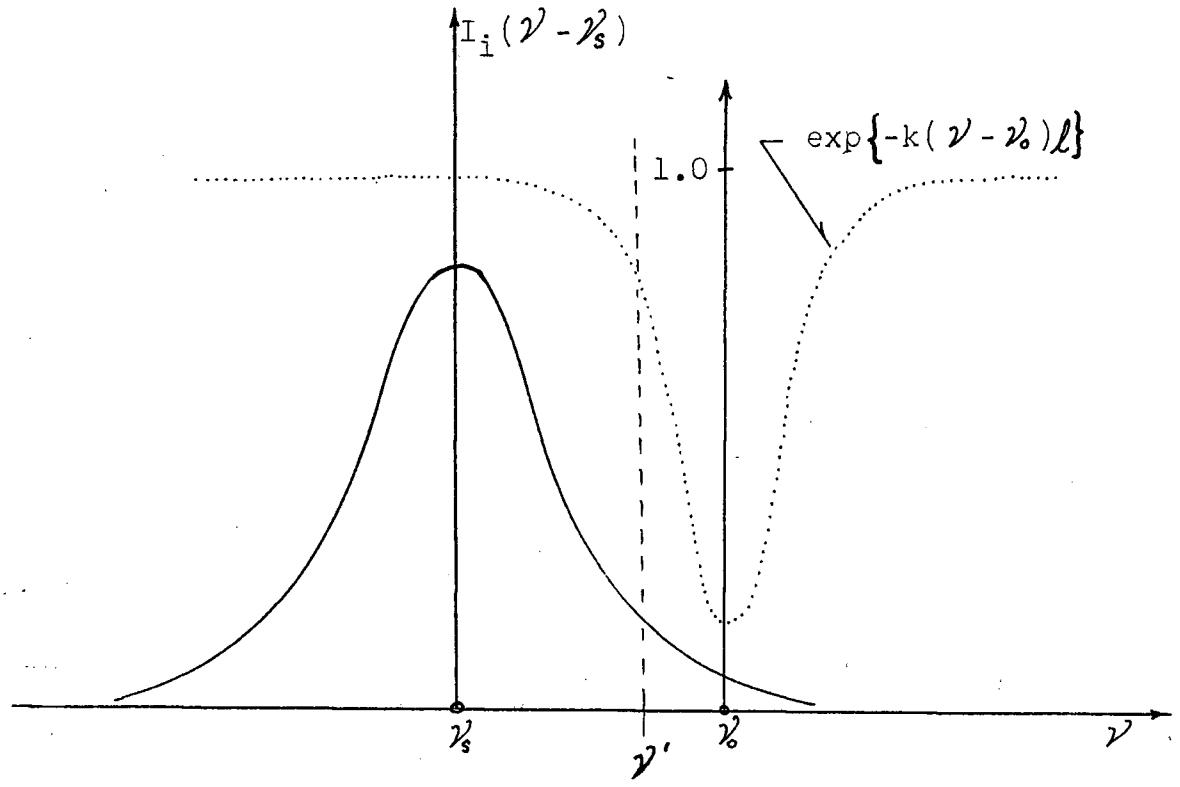

The incident or source flux is: $S(\nu_s) = \int_0^\infty I_i(\nu' - \nu_s)d\nu'$

while the total flux transmitted is: $O(\nu_s, \nu_o) = \int_0^\infty I_f(\nu')d\nu'$

The fractional transmission is the ratio of these two fluxes:

$$t(\nu_s) = \frac{O(\nu_s, \nu_o)}{S(\nu_s)} \qquad \text{IV}$$

Considering the absorber frequency ν_o as a constant the transmission will vary with ν_s, the mean frequency of the source. This is depicted schematically in Fig. 1.

The width of this transmission curve will be defined as the full width at 'half-minimum' - Δt- as indicated in Fig. 1.

Several salient features of such transmission curves are:

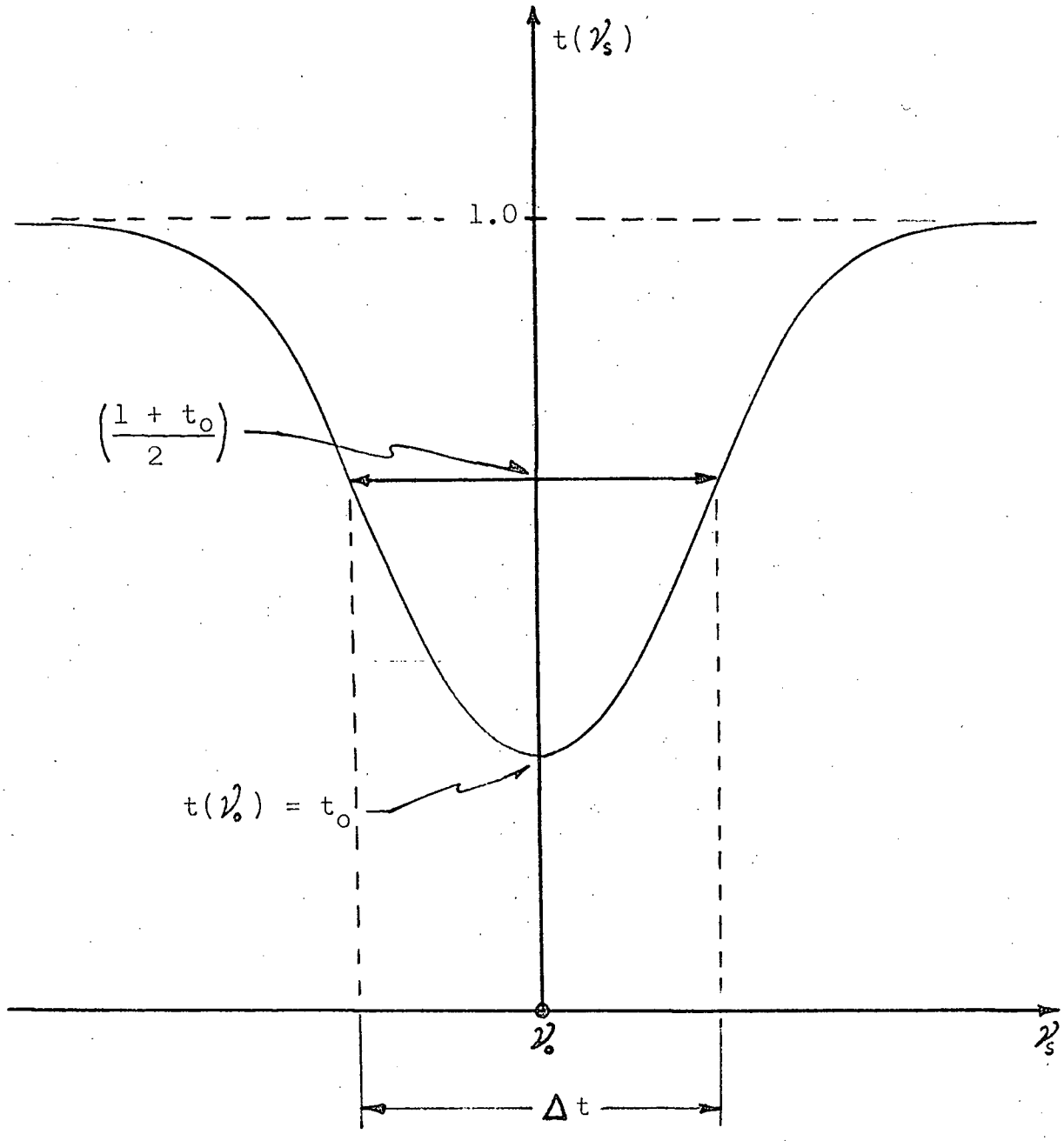

: t_o = line centre (minimum) transmission

: Δt = transmission half width

Fig. 1 Transmission Curve Parameters

(a) For fixed t_o, Δt will increase as the source width and the absorber width increase.

(b) For fixed source and absorber widths, Δt will increase as k_o is increased (i.e. as t_o decreases).

(c) For an infinitely narrow source represented by $I_i(\nu' - \nu_s') = I_o \delta(\nu' - \nu_s')$, then:

$$S(\nu_s') = I_o$$

$$O(\nu_s', \nu_o') = I_o \exp\{ - k(\nu_s' - \nu_o')\ell \}$$

Hence:

$$t(\nu_s') = \exp\{ - k(\nu_s' - \nu_o')\ell \} \qquad \text{IVa}$$

Thus for a sufficiently narrow source $t(\nu_s')$ and Δt depend on the shape of the absorption line only.

B. Line Broadening: Pressure Independent Effects

(1) Natural Broadening:

No spectral line can be perfectly monochromatic. Even an isolated oscillator is still perturbed by the reaction of its own radiation. Classically this can be shown (5) to result in the spectral distribution of intensity:

$$I(\nu - \nu_0) \propto \left[(\nu - \nu_0)^2 + (\frac{1}{2\tau})^2\right]^{-1}$$

where τ is the lifetime of the oscillator.

The half width of this distribution, referred to as the natural line width, is:

$$\Delta\nu_N = \frac{1}{\tau}$$

The normalized intensity is:

$$I(\nu - \nu_0) = \frac{\Delta\nu_N}{2\pi}\left[(\nu - \nu_0)^2 + (\frac{\Delta\nu_N}{2})^2\right]^{-1} \qquad V$$

This inverse square form of frequency dependence was originally derived by H. A. Lorentz in 1906 and has since been named the 'Lorentzian' profile.

The quantum mechanical treatment of this problem yields the same form of intensity distribution and furthermore shows that $\Delta\nu_N$ equals the sum of the spontaneous transition probabilities for all transitions from both the initial and final states. Thus for a line resulting from a transition between states m and n:

$$\Delta\nu_N = \sum_{m'} A_{mm'} + \sum_{n'} A_{nn'}$$

$$= \frac{1}{\tau_m} + \frac{1}{\tau_n}$$

where: $A_{mm'}$ and $A_{nn'}$ are the appropriate Einstein A-coefficients.

τ_m and τ_n are the 'lifetimes' of the two states.

In the optical region the natural line width is usually negligible compared to the effects of other braodening mechanisms. For the $\lambda 6074.3$ A^o line of NeI the lifetime has been measured to be: $\tau \gtrsim 5 \cdot 10^{-7}$ sec (7). This yields a natural width of $\Delta\tilde{\nu}_N \lesssim 6 \cdot 10^{-5}$ cm^{-1}

$= 0.06$ mK.

By comparison the Doppler width (see below) is: $\Delta\tilde{\nu}_D \approx 50$ mK.

(2) Doppler Broadening:

Relative motion between a source of radiation and an observer will cause a frequency shift of the observed radiation (Doppler effect). The random thermal motions of an assemblage of radiation particles will result in a broadening of the spectral line being observed.

For a velocity component along the line of sight v_s, the Doppler frequency shift is:

$$\nu - \nu_o = \pm \frac{v_s}{c} \nu_o$$

where ν_o is the unshifted frequency.

In an assemblage of particles of mass M with a Maxwellian velocity distribution characterized by a temperature T, the fraction with a line of sight velocity component between v_s and $v_s + dv_s$ is:

$$\frac{dN}{N} = \frac{1}{\pi} \exp\left\{ -\left(\frac{M}{2kT}\right) v_s^2 \right\} dv_s$$

N is the total number of particles

k is Boltzmann's constant.

For radiating particles this same fraction will have frequencies between ν and $\nu + d\nu$ where $d\nu = \frac{dv_s}{c} \nu_o$.

Substituting for v_s:

$$\frac{dN(\nu - \nu_o)}{N} = \frac{c}{\pi \nu_o} \exp\left\{ -\frac{Mc^2}{2kT} \left(\frac{\nu - \nu_o}{\nu_o}\right)^2 \right\} d\nu$$

For an optically thin incoherent source the intensity is proportional to the number of radiating particles:

$$\frac{I(\nu - \nu_o)}{I_t} = \frac{dN(\nu - \nu_o)}{N}$$

I_t is the total line intensity.

The half width of this distribution (full width at half-maximum) is:

$$\Delta\nu_o = 2\nu_o \left(\frac{2kT \ln 2}{Mc^2}\right)^{1/2}$$

The normalized intensity distribution is:

$$I(\nu - \nu_o) = \frac{2\sqrt{\ln 2}}{\sqrt{\pi}\,\Delta\nu_o} \exp\left\{ -\left[\frac{2\sqrt{\ln 2}(\nu - \nu_o)}{\Delta\nu_o}\right]^2 \right\} \qquad \text{VI}$$

where $I(\nu - \nu_o)$ is here the intensity at frequency ν per unit frequency interval.

The Doppler frequency shifts arising from thermal motions

thus give the line a Gaussian shape. This is the major broadening mechanism for Geissler tube and glow discharge plasmas such as employed in this experiment. For the $\lambda 6074.3A^{\circ}$ line of NeI (isotope 20) at T = 350 $^{\circ}$K : $\Delta\tilde{\nu}_D = 49$ mK

C. Line Broadening: Pressure Dependent Effects

The perturbations of emitters caused by encounters with surrounding particles result in a further broadening of the spectral line. As pressure and density are increased the rate of such encounters increases, with consequently greater broadening. In this way the broadening is pressure dependent.

(1) Stark Broadening:

During encounters with charged particles the energy levels of an emitter are perturbed (Stark effect). This results in broadened and shifted spectral lines, generally of Lorentzian profile. Compared to ion-broadening, broadening by electrons is generally the greater effect. For low electron densities, such as are encountered in a glow discharge plasma, the effect of the electrons is specifically referred to as 'electron-impact' broadening. The widths and shifts thereby produced are directly proportional to the electron density.

To estimate the significance of this broadening mechanism for the present experiment an estimate of electron density is required. Ecker and Zöller (8) have calculated values for a helium plasma column. Their calculations yield an electron density $n_e \lesssim 10^{11}$ cm^{-3} for pressures, currents, and dimensions

such as employed in this experiment. Assuming that similar values can be expected for a neon discharge, it should be safe to consider $n_e < 10^{12}$ cm^{-3} .

Calculations of the Stark broadening parameters for NeI and other light elements have been performed by Griem (9). From these calculations the electron-impact half width of the λ6074.3 A$^{\circ}$ line of NeI for $n_e < 10^{12}$ cm^{-3} is:

$$\Delta\tilde{\nu}_s < 0.017 \text{ mK}$$

The corresponding shift is: $\Delta\tilde{\nu}_o < 0.009$ mK.

For these calculations the electron temperature was chosen to be 25,000 $^{\circ}$K , the value found by Irwin (10) for a similar neon glow plasma.

Stark broadening of this magnitude is negligible compared with the measured width and such a small shift can not be resolved by the experimental set up.

(2) Van der Waals Broadening and Shift:

The energy levels of an emitter may also be perturbed during encounters with neutral particles. Here also there generally results a broadened and shifted spectral line of Lorentzian profile.

In pure gases the majority of neutral particles encountered by the emitter will be ground state atoms of the same species. In the absence of any resonance effects the interaction forces will be primarily the Van der Waals attraction. For this

the level k is perturbed by: $$\Delta\omega_k = - \frac{C_{6,k}}{r^6}$$

$C_{6,k}$ is the van der Waals constant for the level k and the particular perturber in question.

r is the distance between the radiator and the perturber.

For low density gases such as a glow discharge plasma the impact theory of Lindholm and Foley (11) can quite generally be used. In this theory it is assumed that the duration of the encounter is negligible compared to the time interval between such encounters. This impact approximation is generally valid for low perturber densities such as in typical glow discharge plasmas.

This impact theory, in conjunction with the van der Waals interaction assumed, predicts a Lorentzian intensity distribution whose half width is:

$$\Delta\nu_\nu = 1.3 v^{3/5} C_6^{3/5} n \text{ sec}^{-1} \qquad \text{VII}$$

v is the mean relative velocity between emitter and perturber.

$C_6 = C_{6,k} - C_{6,k'}$ where k' and k designate the initial and final levels.

n is the number density of the perturbers.

In addition to the broadening the impact theory also predicts a shift of the spectral line to the red. The ratio of broadening to shift is independent of both the interaction constant C_6 and the mean relative velocity v. For a width $\Delta\nu_\nu$

the shift is: $\Delta\nu_o = -\frac{\Delta\nu_r}{2.76}$

The van der Waals constants may be estimated using the following approximation by Unsöld (12) :

$$C_{6,k} = \frac{e^2}{\hbar}\alpha_p \frac{a_o^2}{2} n^{*2}\left[5n^{*2} + 1 - 3\ell(\ell+1)\right] \text{ rad sec}^{-1}\text{cm}^6 \qquad \text{VIII}$$

e is the electronic charge.

$\hbar$ is Planck's constant for angular momentum.

a_o is the first Bohr radius.

n^* is the effective quantum number of the level k.

ℓ is the angular momentum quantum number for the optical electron in level k.

α_p is the polarizability of the <u>perturbing</u> particles.

The validity of this approximation rests on the assumption that the energy separation between the initial and final levels of the emitter is much smaller than the energy separation of the ground state and lower excited states of the perturber (for ground state perturbers). This is a reasonable assumption for a noble gas perturber since there the first excited states lie comparatively high as a result of the increase in principal quantum number of the optical electron. Hence Unsöld's approximation VIII should be valid for neon in a glow discharge plasma.

The application of Unsöld's approximation requires an

estimate of the polarizability α_p of neon. Two values of this have been utilized. The first, a theoretical value, has been taken from Allen (13) who gives $\alpha_p = 3.96 \cdot 10^{-25}$ cm^3. Using the Unsöld approximation VIII this yields:

$$C_{6(Ne6074/Ne)} = 5.82 \cdot 10^{-32} \text{ rad sec}^{-1} \text{ cm}^6$$

Hence from the impact theory relation VII :

$$\frac{\Delta\tilde{\nu}}{n} = \frac{1}{c} \frac{\Delta\nu}{n} = 1.24 \cdot 10^{-17} \text{ mK cm}^3$$

Secondly, an experimentally based value has been derived from the results of Smith (14) on the pressure broadening of Ca λ6573 A$^\circ$ by neon. Smith's quoted value of $\frac{\Delta\tilde{\nu}}{n} = 11.0 \cdot 10^{-18}$ mK cm^3 and relation VII yield:

$$C_{6(Ca6573/Ne)} = 2.27 \cdot 10^{-32} \text{ rad sec}^{-1} \text{ cm}^6$$

This Ca λ6573 A$^\circ$ line is a 4s4p - 4s^2 transition and the energy separation of the initial and final states is roughly equal to that of the Ne λ6074.3 A$^\circ$ line. Hence the Unsöld approximation VIII should be equally valid in this case. Using relation VIII then, the polarizability of neon was derived and from this:

$$C_{6(Ne6074/Ne)} = 1.26 \cdot 10^{-31} \text{ rad sec}^{-1} \text{ cm}^6$$

With relation VII again this yields:

$$\frac{\Delta\tilde{\nu}}{n} = 1.69 \cdot 10^{-17} \text{ mK cm}^3 .$$

For a plasma with T $\simeq$ 325 $^\circ$K and P = 10 Torr (typical for

glow discharges) the neutral particle density $n \simeq 3 \cdot 10^{17}$ cm^{-3}. Under such conditions the above results predict van der Waals half widths for the Neλ6074.3 A$^{\circ}$ line of:

$$\Delta\tilde{\nu}_v \simeq 3.7 \text{ mK (theory)}$$
$$\Delta\tilde{\nu}_v \simeq 5.1 \text{ mK (from Smith (14))}$$

Since this is 8 - 10 % of the Doppler width for the same conditions, van der Waals pressure broadening could substantially affect line shapes in a glow discharge. The experimental results confirm this expectation.

The impact theory with van der Waals interaction also predicts a corresponding line shift of:

$$\Delta\tilde{\nu}_o \simeq 1.8 \text{ mK to the red.}$$

However a shift of this magnitude would be barely detectable, if at all, with the experimental apparatus employed. However the larger shifts to be expected at the higher pressures used should be easily detected.

The shift of the Ca λ6573 A$^{\circ}$ line broadened by neon observed by Smith (14) was not only smaller by a factor of 15 than the prediction of the impact theory but was in addition to the blue. This failure of the theory was attributed by Hindmarsh, Petford, and Smith (15) to the omission of any repulsive force in the interaction assumed. Similar results should obtain for the shift of the Ne λ6074.3 A$^{\circ}$ line in which case the actual shifts produced would be beyond detection with the experimental apparatus.

D. Self Absorption Broadening

The broadening mechanisms discussed in Sections B and C act to broaden a spectral line 'as it is emitted' and result from the immediate physical environment of the emitting particles. These mechanisms apply to both the emission and absorption processes.

Subsequent transmission through an absorbing medium may further affect the intensity distribution of the emitted light. Since any practical light source must be composed of many emitting particles, some of the light originating from regions most distant from an observer may be partially absorbed before emerging from the volume of the source. Consequently the resultant frequency distribution of intensity from the source as a whole may differ from that of the emitting particles per se.

Consider a homogenous source of dimension ℓ in the line of observation. Let the emissivity per unit length be $j(\nu - \nu_0)$, where ν_0 is the spectral line centre, and let the absorption constant (as defined in Section A) be $k(\nu - \nu_0)$.

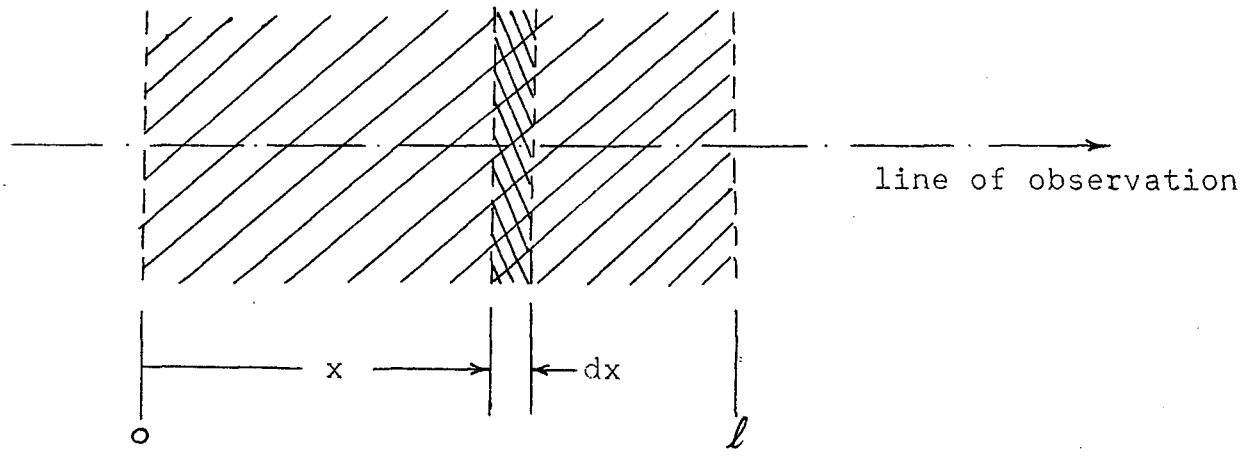

In the absence of any absorption the emergent intensity at frequency ν would be $I_\ell(\nu-\nu_0) = j(\nu-\nu_0)\ell$.

The intensity emitted by the element dx at frequency ν is similarly : $j(\nu-\nu_0)dx$. The amount of this which emerges at ℓ is given by III :

$$dI_s(\nu-\nu_0) = j(\nu-\nu_0)\exp\left\{-k(\nu-\nu_0)\left[\ell - x\right]\right\} dx$$

The net intensity is found by integrating over the source:

$$I_s(\nu-\nu_0) = \int_0^\ell dI_s(\nu-\nu_0)$$

$$= \frac{j(\nu-\nu_0)}{k(\nu-\nu_0)}\left[1 - \exp\left\{-k(\nu-\nu_0)\ell\right\}\right]$$

The quantity in the exponent is defined as the optical depth : $\tau(\nu-\nu_0) = k(\nu-\nu_0)\ell$

$$I_s(\nu-\nu_0) = \frac{I_\ell(\nu-\nu_0)}{\tau(\nu-\nu_0)}\left[1 - \exp\left\{-\tau(\nu-\nu_0)\right\}\right] \qquad \text{IX}$$

An optically thin source is one in which any photon emitted has a high probability of escaping (i.e. avoiding absorption). The criterion for optical thinness at frequency ν is : $\tau(\nu-\nu_0) \ll 1$.

For an optically thin source :

$$I_s(\nu-\nu_0) \simeq \frac{I_\ell(\nu-\nu_0)}{\tau(\nu-\nu_0)}\left[1 - (1 - \tau(\nu-\nu_0)\right]$$

$$= I_\ell(\nu-\nu_0)$$

From this it can be seen that in the optically thin case the line profile of the emitted light is unaffected.

For an optically thick source (but one in which $\tau(\nu-\nu_0) \leq 1$ still) :

$$I_s(\nu-\nu_0) \simeq \frac{I_\ell(\nu-\nu_0)}{\tau(\nu-\nu_0)}\left[1 - (1 - \tau(\nu-\nu_0) + \frac{\tau(\nu-\nu_0)^2}{2} \ldots\ldots)\right]$$

$$= I_\ell(\nu-\nu_0)\left[1 - \frac{\tau(\nu-\nu_0)}{2} + \ldots.\right]$$

Since $\tau(\nu-\nu_0)$ is greatest for the centre of the line ($\nu \simeq \nu_0$) the line core is self absorbed more strongly than the wings. As a result the apparent half width of the line increases:

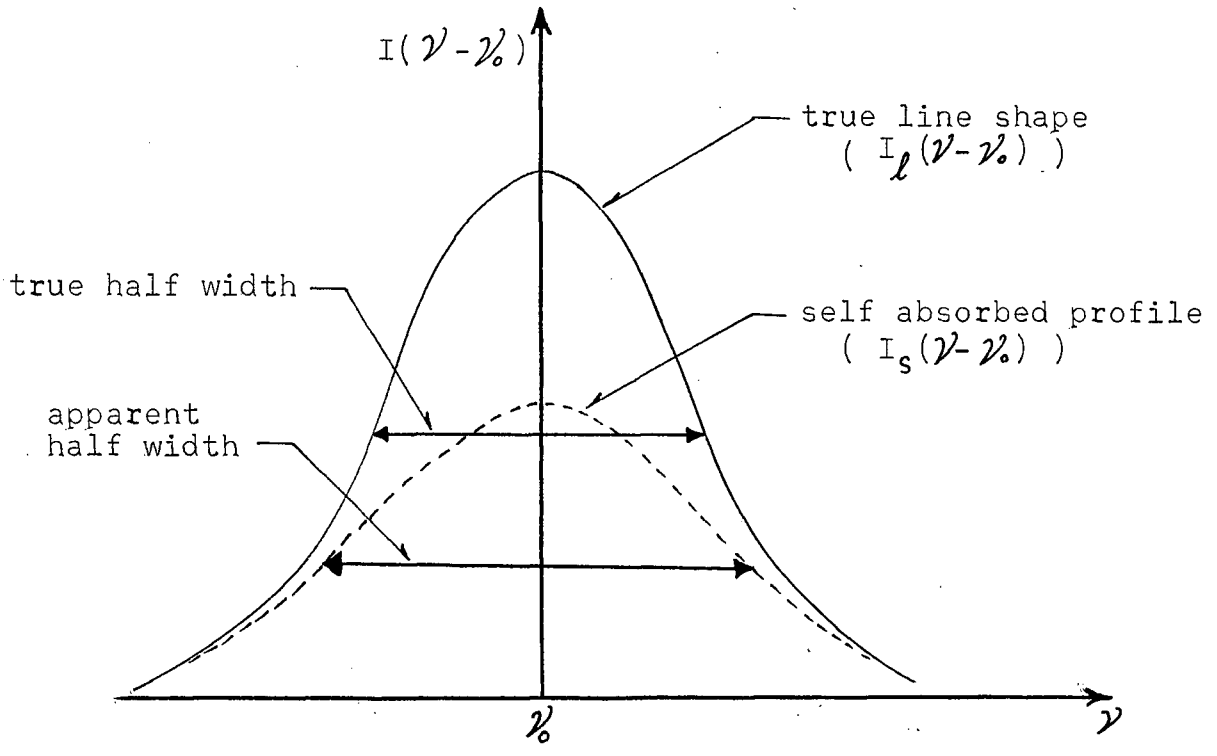

E. Voigt Profiles

Where two different mechanisms act independently to broaden a line the resultant line profile is the convolution of their two shapes. If $S_1(\nu - \nu_o)$ is the profile due to one mechanism and $S_2(\nu - \nu_o)$ is the profile due to the other, then one considers each element of the S_1 profile to be broadened with an S_2 shape. The resultant intensity at any frequency ν_s is the sum of all the contributions from each broadened element of S_1.

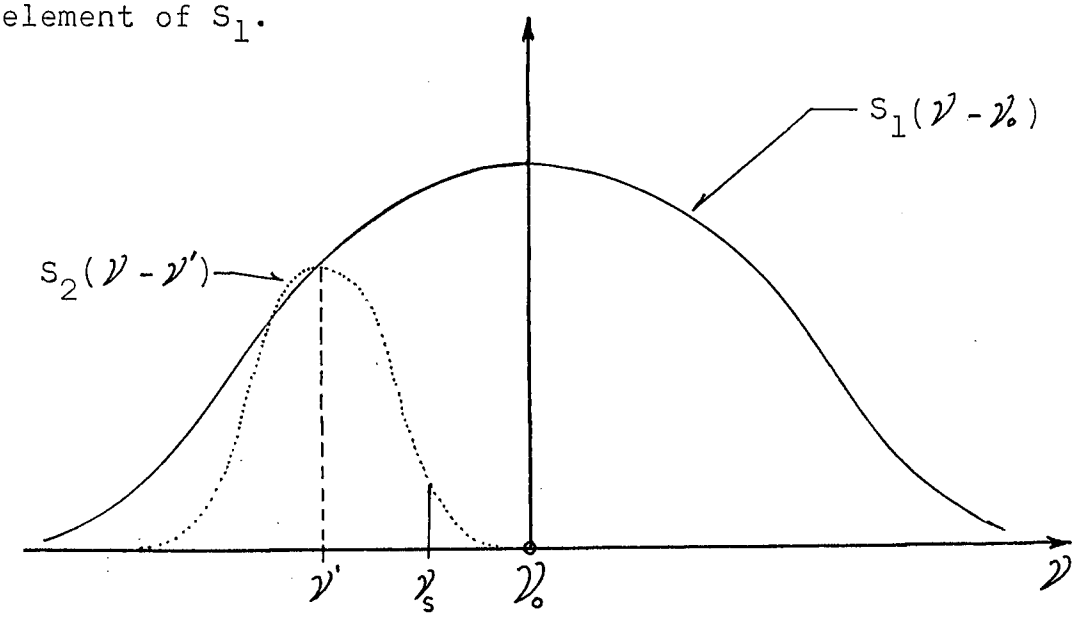

$$S(\nu_s - \nu_o) = \int_o^\infty S_1(\nu' - \nu_o) \cdot S_2(\nu_s - \nu') d\nu' \qquad X$$

Setting $\nu_s - \nu_o = x$ and $\nu' - \nu_o = y$ one obtains the more familiar form:

$$S(x) = \int_o^\infty S_1(y) \cdot S_2(x - y) dy$$

If S_1 is Gaussian and S_2 Lorentzian (or vice versa) their convolution is defined as a Voigt profile. It can be shown (16) that if S_1 and S_2 are themselves Voigt profiles then their convolution S will also be a Voigt profile. Furthermore, should S_1 be formed from a Gaussian of half width $\Delta\nu_{D1}$ and a Lorentzian of half width $\Delta\nu_{L1}$, while S_2 results from a Gaussian of half width $\Delta\nu_{D2}$ and a Lorentzian of half width $\Delta\nu_{L2}$, S is then the Voigt profile resulting from a Gaussian of half width $\Delta\nu_D$ and a Lorentzian of half width $\Delta\nu_L$ such that:

$$\Delta\nu_D^2 = \Delta\nu_{D1}^2 + \Delta\nu_{D2}^2$$

$$\Delta\nu_L = \Delta\nu_{L1} + \Delta\nu_{L2}$$

The Gaussian and Lorentzian profiles are themselves extreme cases of Voigt profiles. Consequently, if two broadening mechanisms, each of which produces a Lorentzian profile, act independently then the resultant line shape will be Lorentzian. For example, should van der Waals broadening and Stark broadening both be significant, their joint result will be a Lorentzian profile with a half width of:

$$\Delta\nu_L = \Delta\nu_s + \Delta\nu_v$$

Substituting in equation X the Gaussian of VI for S_1 and the Lorentzian of V for S_2 (with half widths $\Delta\nu_D$ and $\Delta\nu_L$ respectively):

$$S(\nu_s - \nu_o) = \int_0^\infty \left[\frac{2\sqrt{\ln 2}}{\sqrt{\pi}\,\Delta\nu_D} \exp\left\{-\left[\frac{2\sqrt{\ln 2}\,(\nu' - \nu_o)}{\Delta\nu_D}\right]^2\right\}\right] \times \left[\frac{\Delta\nu_L}{2\pi}\left[(\nu_s - \nu')^2 + \left(\frac{\Delta\nu_L}{2}\right)^2\right]^{-1}\right] d\nu'$$

Setting $x = \frac{2\sqrt{\ln 2}}{\Delta\nu_D}(\nu' - \nu_o) = F(\nu' - \nu_o)$

$$dx = F d\nu'$$

$$\nu_s - \nu' = \nu_s - \nu_o - (\nu' - \nu_o)$$

$$= \nu_s - \nu_o - \frac{x}{F}$$

$$S(\nu_s - \nu_o) = \frac{\Delta\nu_L}{2\pi^{3/2}} \int_{-\infty}^{\infty} \frac{\exp\{-x^2\}}{(\nu_s - \nu_o - \frac{x}{F})^2 + (\frac{\Delta\nu_L}{2})^2} dx$$

$$= \frac{F\,\Delta\nu_L}{2\pi^{3/2}} \int_{-\infty}^{\infty} \frac{\exp\{-x^2\}}{(F(\nu_s - \nu_o) - x)^2 + (\frac{F\Delta\nu_L}{2})^2} dx$$

Setting $\frac{F\Delta\nu_L}{2} = \frac{2\sqrt{\ln 2}\,\Delta\nu_L}{2\Delta\nu_D} = A\sqrt{\ln 2} = Y$

$$S(\nu_s - \nu_o) = \frac{Y}{\pi^{3/2}} \int_{-\infty}^{\infty} \frac{\exp\{-x^2\}}{(F(\nu_s - \nu_o) - x)^2 + Y^2} dx \qquad \text{XI}$$

The ratio of Lorentzian to Gaussian half width: $A = \frac{\Delta\nu_L}{\Delta\nu_D}$ is termed the Voigt A-parameter. It specifies the shape of the Voigt profile.

$A = 0$ - pure Gaussian

$A \to \infty$ - pure Lorentzian

Values of the Voigt integral of equation XI required for transmission curve calculations were computed using a Fortran IV subprogramme developed at the University of Michigan (17).

F. Zeeman Scanning and Inhomogeneity Broadening

The major group of visible neon spectral lines results from $2p^5 3p \rightarrow 2p^5 3s$ transitions. While most of these lines exhibit complex (anomalous) Zeeman patterns in a magnetic field, several show the normal Zeeman pattern required for Zeeman scanning. The λ6074.3 A^o line, which results from a $^3P_0 \rightarrow {}^3P_1$ transition, is one of these (see Figure 2).

The splitting $\delta\tilde{\nu}(cm^{-1})$ is given (18) by:

$$\delta\tilde{\nu} = \pm gHB \qquad \text{XII}$$

where B is the applied magnetic field (gauss).

$H = 4.695 \cdot 10^{-5}$ $cm^{-1} gauss^{-1}$ (the Zeeman constant).

g is the splitting factor for the line.

(g = 1.45 for Ne λ6074.3 A^o (18))

Zeeman scanning is effected by placing the source in a variable magnetic field. A beam is taken in the direction of the field (longitudinally). This beam contains only the two σ - components of the normal Zeeman triplet, which are right - and left - hand circularly polarized respectively. A quarter wave plate converts these to mutually perpendicular linearly polarized beams. An analyzing Nicol prism then suppresses one of these two beams. As the magnetic field varies the Zeeman shift, and hence the frequency ν_s, of the remaining beam varies.

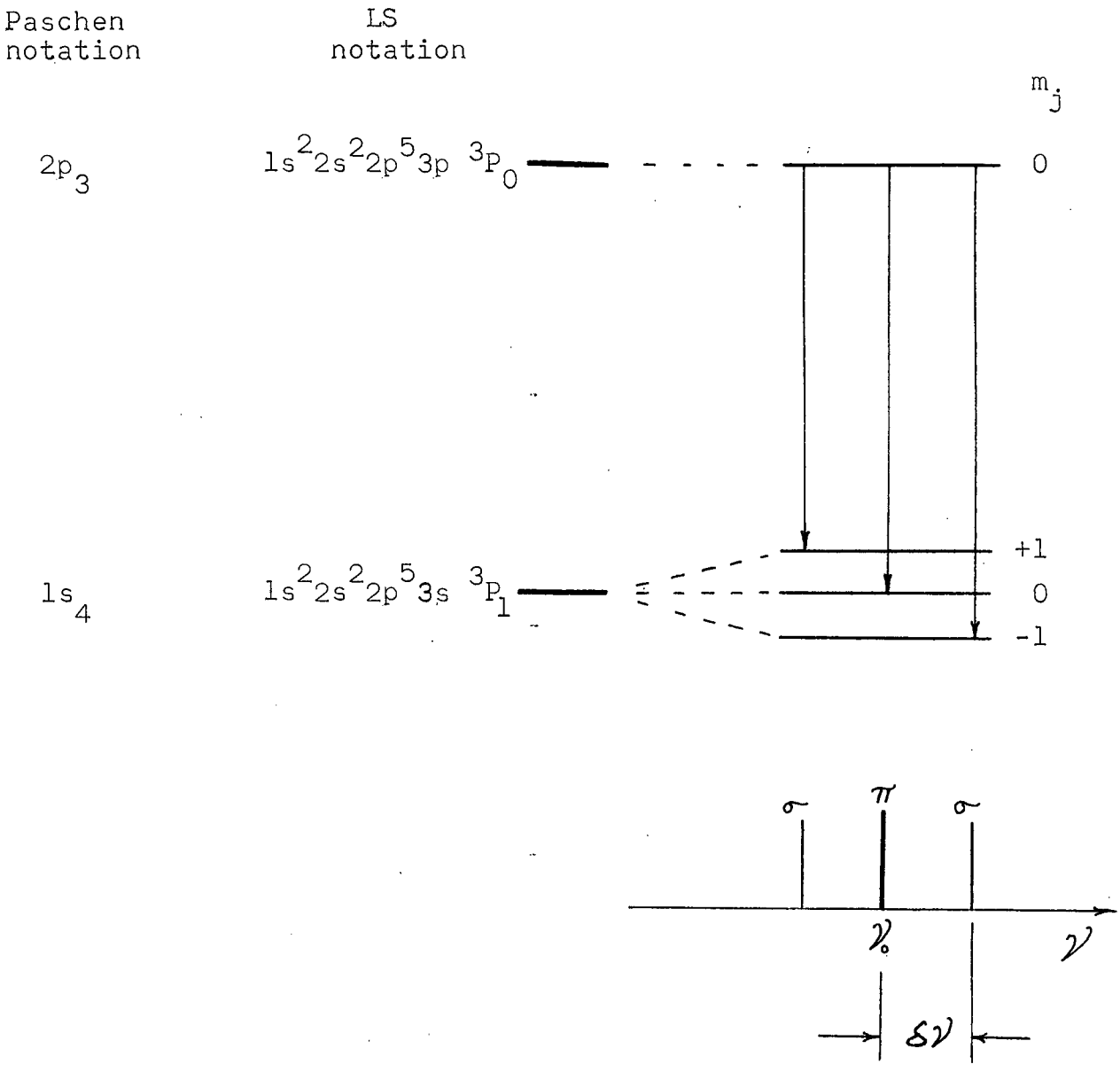

Fig. 2 Spectroscopic Designation and Zeeman Effect for Ne λ6074.3 $\mathring{A}$

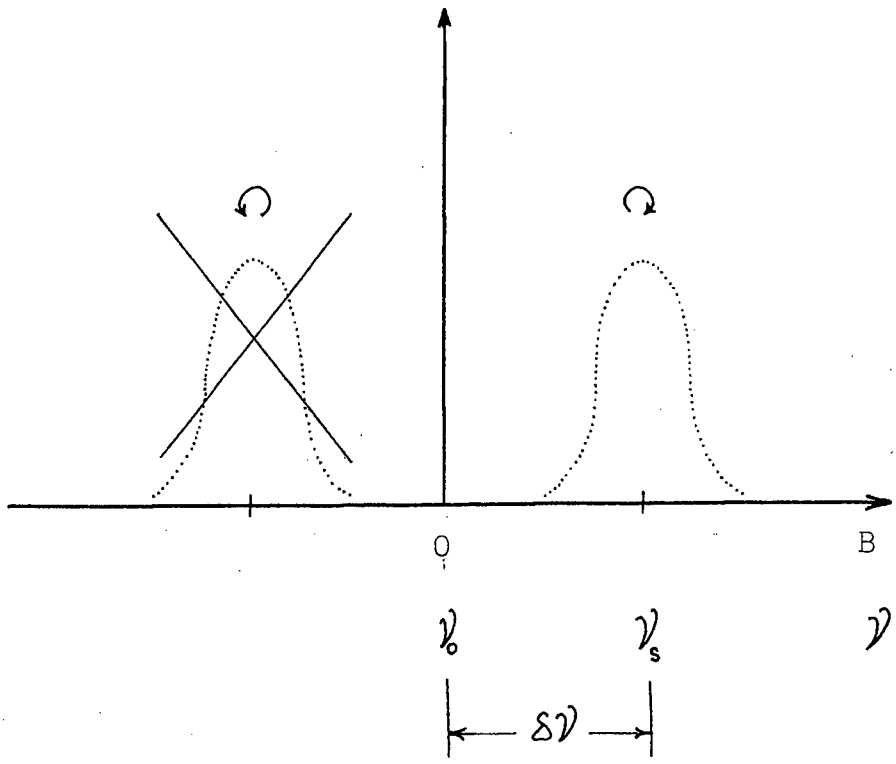

This technique provides a single spectral line of variable frequency, this frequency being determined by equation XII in conjunction with the orientation of the Nicol prism and the sense of the magnetic field.

If the magnetic field is not homogeneous over the volume of the source then the source line shape may be distorted. Contributions from regions with slightly different magnetic field strengths would have correspondingly different frequency shifts. The resultant line profile would thus appear broadened and possibly asymmetric.

This field inhomogeneity broadening will increase with magnetic field strength. The effect would thus be greatest for measurements of the wings of the absorption line.

CHAPTER III

APPARATUS

A. Source

A neon Geissler tube filled to 2 Torr pressure served as the source. The gas was isotopically pure Ne20 with a 0.6 Mol. % hydrogen impurity.

The outer surface of the capillary section was coated with black enamel paint except for a small aperture of 1 mm diameter. The capillary itself had a diameter of 1 mm so that the source volume was approximately one cubic millimetre.

The tube was operated from a 1000 volt regulated supply at a current of 4 ma. The current was controlled by a series pentode and ballast resistor. The discharge was initiated with a Tesla coil.

B. Scanning Electromagnet

The Geissler tube source was centrally positioned between the poles of an electromagnet. The pole pieces were hollow centred with the central hole tapering to 3 mm diameter nearest the source.

Magnetic field strength versus electromagnet current calibration for the field at the source position was obtained using a Bell Model 240 gaussmeter (a Hall probe instrument).

Measurements of field inhomogeneity indicate no field

gradients greater than 3% per cm in the central region. Over 1 mm (the characteristic length of the source) there is less than 0.3% variation. The maximum Zeeman shift required was 0.4 cm^{-1} , in which case this inhomogeneity results in shift differences of not more than 1.2 mK. Since this is less than 3% of the source half width, and since the field strength was usually much lower than this, field inhomogeneity broadening was not considered significant in this experiment.

C. Absorption Tubes

The absorber was a hollow cathode glow discharge in isotopically pure Ne20 (also with the 0.6 Mol. % hydrogen impurity). The source beam was passed through the hollow cathode.

Absorption tubes of three different filling pressures, 2 Torr, 50 Torr, and 100 Torr, were employed. The discharge in all three tubes was maintained by a 1400 volt regulated supply with the current controlled by a series pentode and ballast resistor. The ballast was made as large as possible in order to reduce current fluctuations. The discharge usually had to be initiated with a Tesla coil.

Different absorption strengths were obtained by varying the current between 0.3 ma and 16 ma.

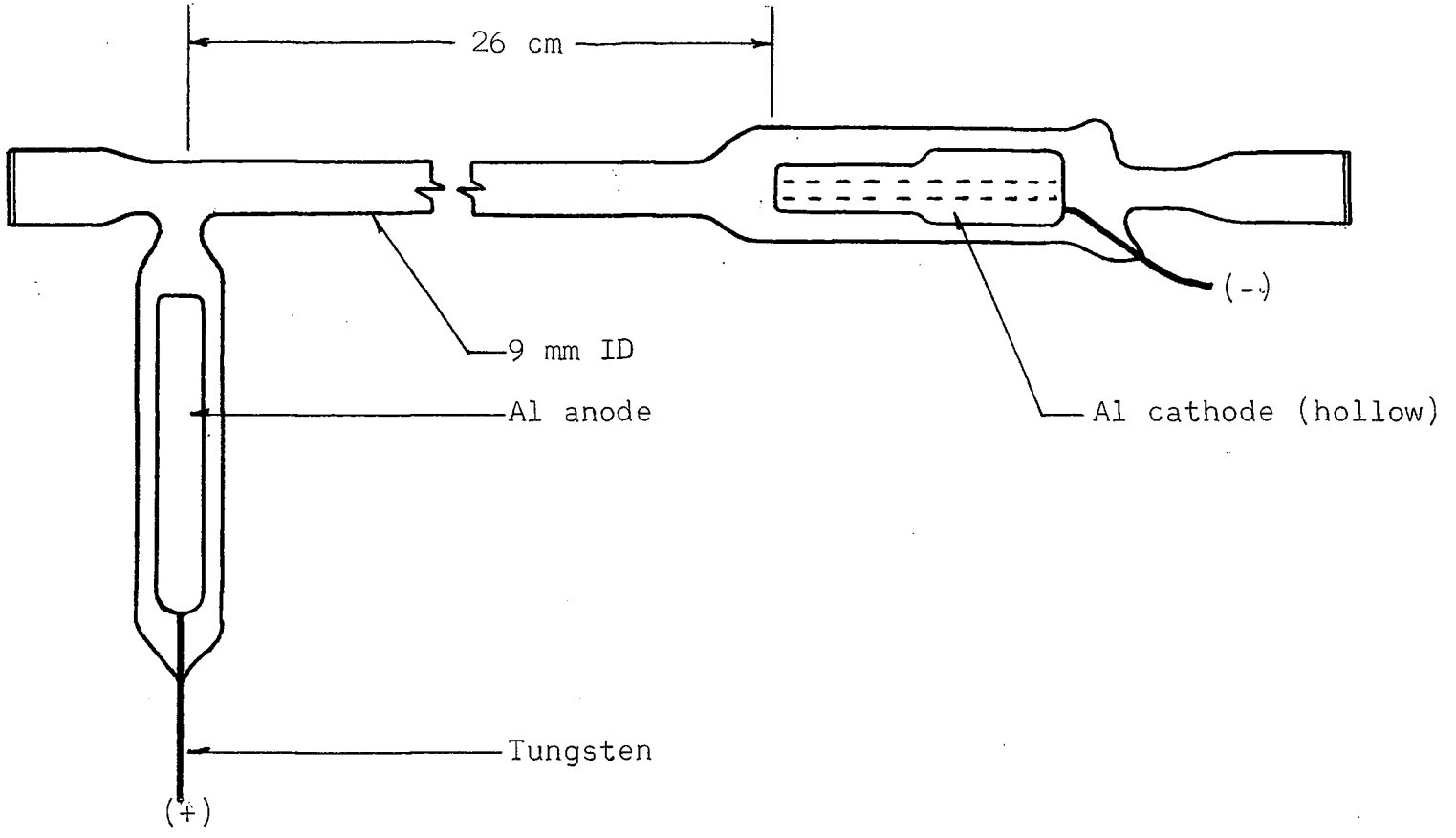

Fig. 3 Absorption Tube Construction

D. Optical System

The beam emergent from the magnet was rendered parallel by lens L_1 (see Fig. 4). After amplitude modulation at 990 Hz by the chopping wheel it passed into the absorber through the hollow cathode. The small cathode bore (3 to 5 mm ID), along with a 3 mm diameter stop placed on the exit end of the absorption tube, ensured that only a small relatively homogeneous region in the centre of the absorption tube attenuated the beam.

Next followed the quarter wave plate and the analyzing Nicol prism. These were placed after the absorber so that they also served to suppress part of the 'noise' emission from the absorber.

The second lens L_2 focussed the beam onto the entrance slit of a 500 mm Bausch and Lomb grating monochromator of low dispersion. The entrance slit and stops were opened just wide enough to accept all the source beam. The exit slit was opened sufficiently wide to easily accept the entire spectral line but yet kept narrow enough to still exclude any nearby spectral lines. The light emerging from the monochromator was converted to electrical current by a Phillips 150 CVP Photomultiplier operated at approximately 1500 volts and cooled by dry ice.

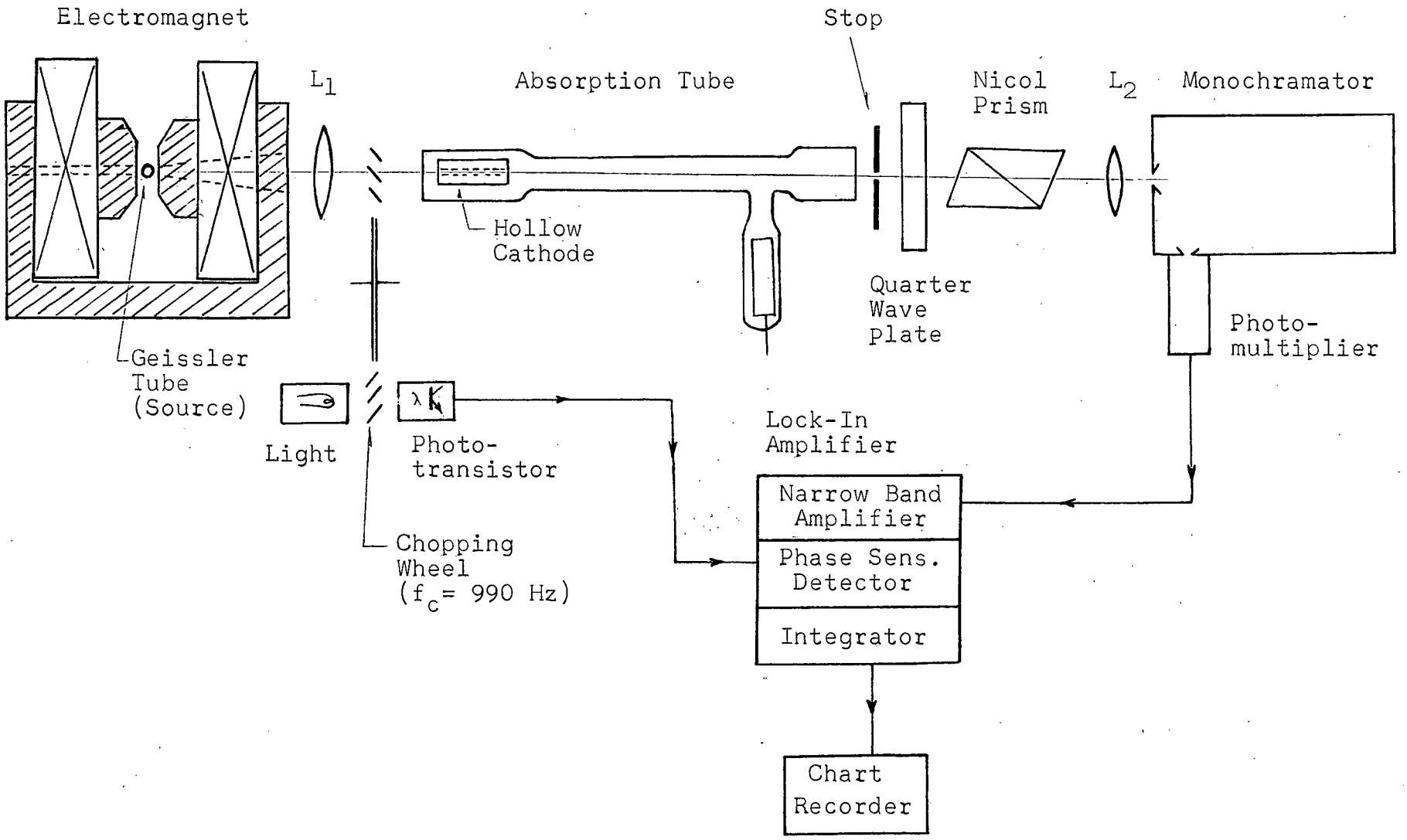

Fig. 4 Experimental Arrangement

E. Electronic Detection

Conditions in the absorption tubes fluctuated, causing fluctuations both in the radiation emitted and the absorption strength. In order to achieve a satisfactory signal to noise ratio it was necessary to employ phase sensitive detection and signal integration.

The photomultiplier signal was sent to a Princeton Applied Research Lock-In Amplifier (Model 120). Essentially this device is a narrow band amplifier tuned to the chopper frequency of 990 Hz followed by a phase sensitive detector. A signal produced by the chopping wheel with a light and a photo-sensitive transitor supplied the phase reference.

The d.c. signal produced was fed to an RC integrating network (incorporated in the Lock-In Amplifier). Time constants from 0.3 sec to 3 sec were employed depending upon the noise encountered. The output was monitored on a Heathkit Chart Recorder (Model EUW - 20A).

CHAPTER IV

EXPERIMENTAL PROCEDURE

The optical system was initially aligned on the beam of a continuous He-Ne laser shone into the exit slit of the monochromator. Final alignment was accomplished by minor adjustments to the source position, the absorption tube position, and the position of the lens L_2 such that a maximum signal was obtained.

The direction of the frequency shift (the sign in equation XII) was determined by substituting a source of natural neon. The presence of the Ne22 isotope caused an asymmetry in the transmission curve from which the direction of the shift could be deduced.

Each transmission curve was obtained by varying the electromagnet current monotonically and in discrete steps. For each current value, and hence each source frequency, the transmitted line intensity was measured both with the absorbing discharge switched on and off. The ratios of these two intensities yields the fractional transmission t_o. The source frequency was obtained by converting the electromagnet current value to the corresponding magnetic field strength using the magnet calibration and then substituting into equation XII.

With each absorption tube the transmission curves were obtained for a range of absorption strengths by varying the absorption tube current from experiment to experiment.

CHAPTER V

METHOD OF ANALYSIS

A. Choice of Model

The shape of the absorption line cannot be directly obtained from a transmission curve. It is necessary to consider models in which the exact profiles of the source and the absorber are specified and from these to compute theoretical transmission curves. The model which produces the closest approximation to the experimental result is then considered to describe the absorption line.

Unfortunately this procedure may not yield a unique result. However, if it be assumed that the shape of the absorption line does not change as the absorption strength k_o is varied (by altering the absorber current), then the variation of the transmission profiles with absorption strength offers an additional constraint on the model. This enables a choice to be made from an initial set of models.

The spectral lines of source and absorber were both considered to be described by Voigt profiles. Their Gaussian half widths were assumed to result solely from Doppler broadening. Since the Geissler tube capillary was slightly warmer than the absorption tube and since both were warmer than room temperature, it could be assumed:

(a) $T_s > T_a$

(b) $T_a > 300\ ^{o}K$

where T_s and T_a are the source and absorber temperatures respectively.

The Lorentzian half widths were assumed to result entirely from pressure broadening. Consequently the lines of the 2 Torr pressure absorber could be assumed to have the same Lorentzian half width ($\Delta\nu_{LS}$) as the source.

The source was considered further broadened by self absorptian. For an intrinsic Voigt shape $S(\nu - \nu_s)$ the self absorbed shape was taken as :

$$I_i(\nu - \nu_s) \propto \left[1 - \exp\{ - K \cdot S(\nu - \nu_s)\} \right]$$

This results from equation IX under the assumption that $j(\nu - \nu_s)$ and $k(\nu - \nu_s)$ have the same frequency dependence.

The higher pressure absorbers were assumed to have the same temperature as the 2 Torr pressure absorber since their tubes were not noticeably warmer during operation than the 2 Torr tube. The transmission curves for these absorbers provide a further test for the models.

B. Specific Procedure

(1) An assignment of T_s, T_a, $\Delta\nu_{LS}$, and K was made.

(2) The absorption strength $k(0)\ell$ was varied until a line centre transmission t_o of 0.33 was obtained.

(3) The full transmission curve was calculated, plotted, and then compared with the experimental results for the 2 Torr absorber in which t_o equalled 0.33.

(4) The parameters (T_s, T_a, $\Delta\nu_{LS}$, K) were varied until

an acceptable fit was obtained.

(5) Transmission curves for $t_o = 0.16$ and $t_o = 0.53$ were then calculated for these parameters and compared to the corresponding experimental results (see Figure 8).

(6) A graph of transmission half width (Δt) versus t_o was computed for a range of values of the absorber Lorentzian half width. These were then compared with the experimental results for all three pressures (see Figure 10).

(7) Finally transmission curves for the indicated absorber Lorentzian half widths of the 50 Torr and 100 Torr pressure absorbers were computed for $t_o = 0.33$ and compared to the corresponding experimental results (see Figure 9).

By repeated trial and error a set of parameters (T_s, T_a, $\Delta\nu_{ls}$, K) was obtained which satisfied all these checks and tests. In addition a Lorentzian half width was thereby assigned for each absorber pressure.

CHAPTER VI

RESULTS

A. Detection of Broadening

Broadening can be detected by comparing the transmission curves for absorption tubes of different filling pressures. In cases where the line centre transmissions t_o are equal such comparisons clearly demonstrate the pressure broadening of the absorption line. Figures 5, 6, and 7 on the next three pages show experimental results for t_o = 0.16, 0.33, and 0.53 respectively. In terms of transmission curve half widths (Δt) these results are summarized below:

t_o	Δt(mK)		
	2 Torr	50 Torr	100 Torr
0.16	106	123	144
0.33	91	109	132
0.53	87	98	121

Width variations less than those observed here could still be detected. Experience indicated that curves with a fifth of such width differences could still be unambiguously distinguished. In section C following it will be seen that from 2 Torr to 100 Torr there was an increase in the Lorentzian half width of the absorbers of approximately 45 mK. Hence study of the transmission curves would enable an increase in the absorber half width of as little as 5 mK to be detected.

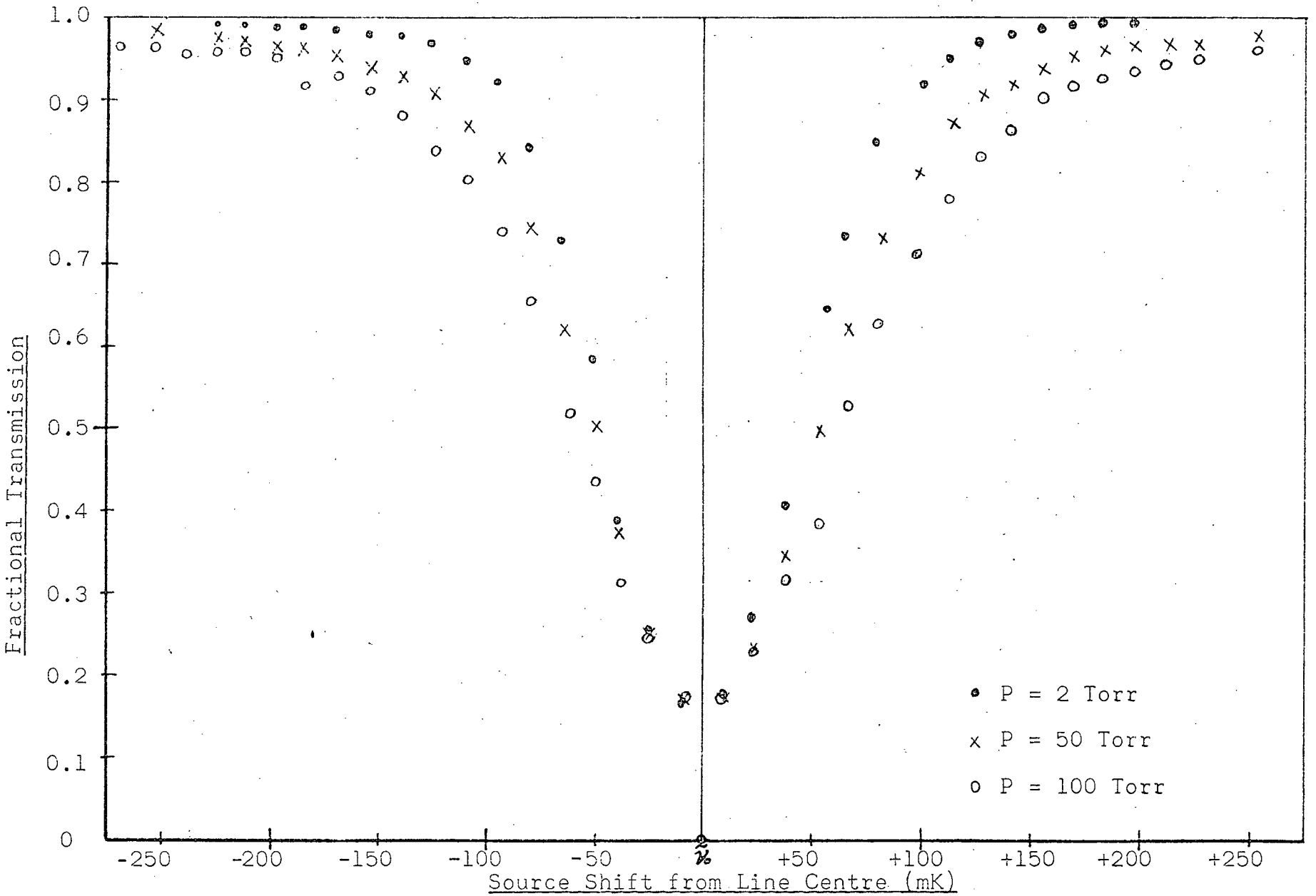

Fig. 5 Transmission Curves for Different Pressures (t_o = 0.16)

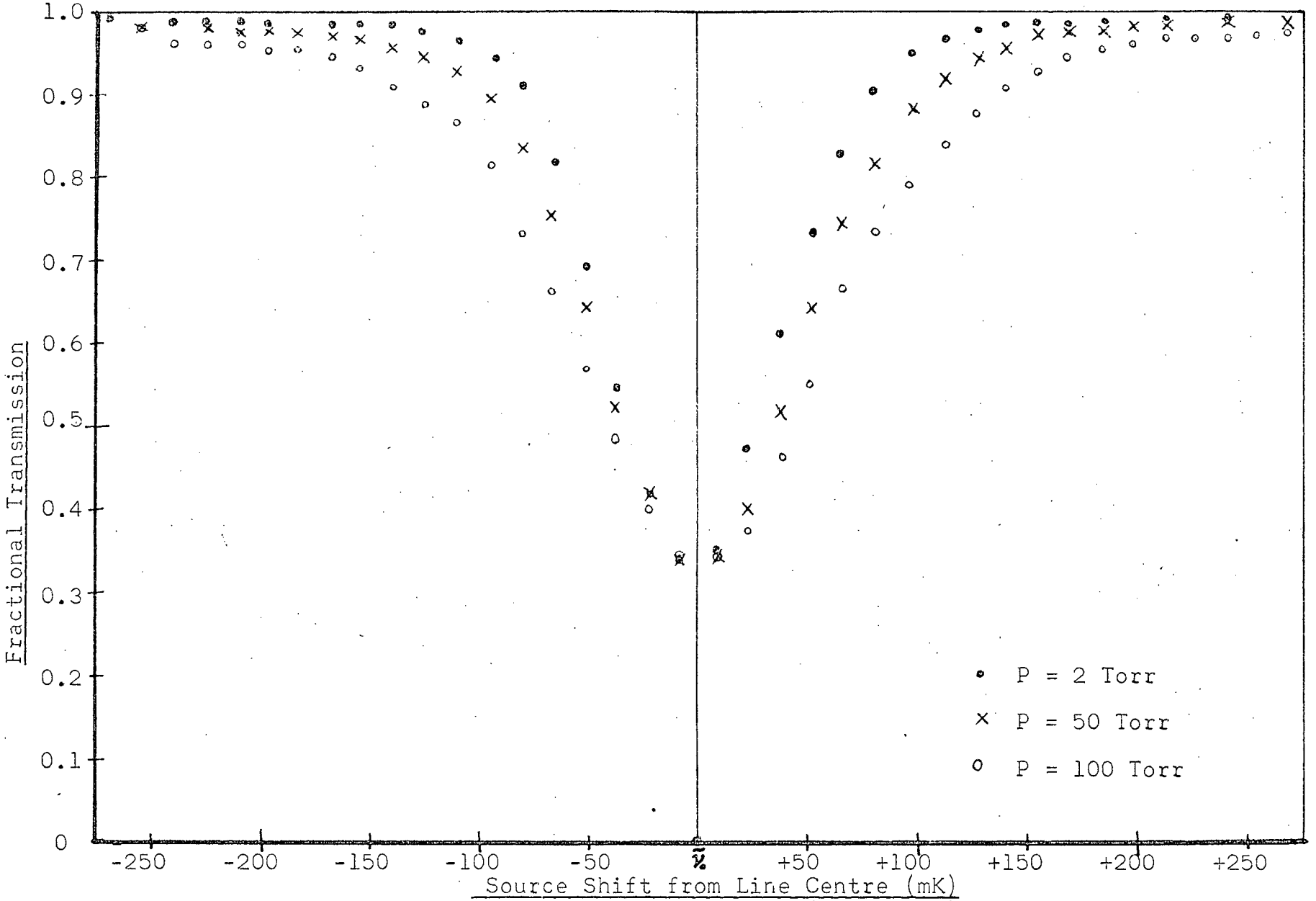

Fig. 6 Transmission Curves for Different Pressures (t_o = 0.33)

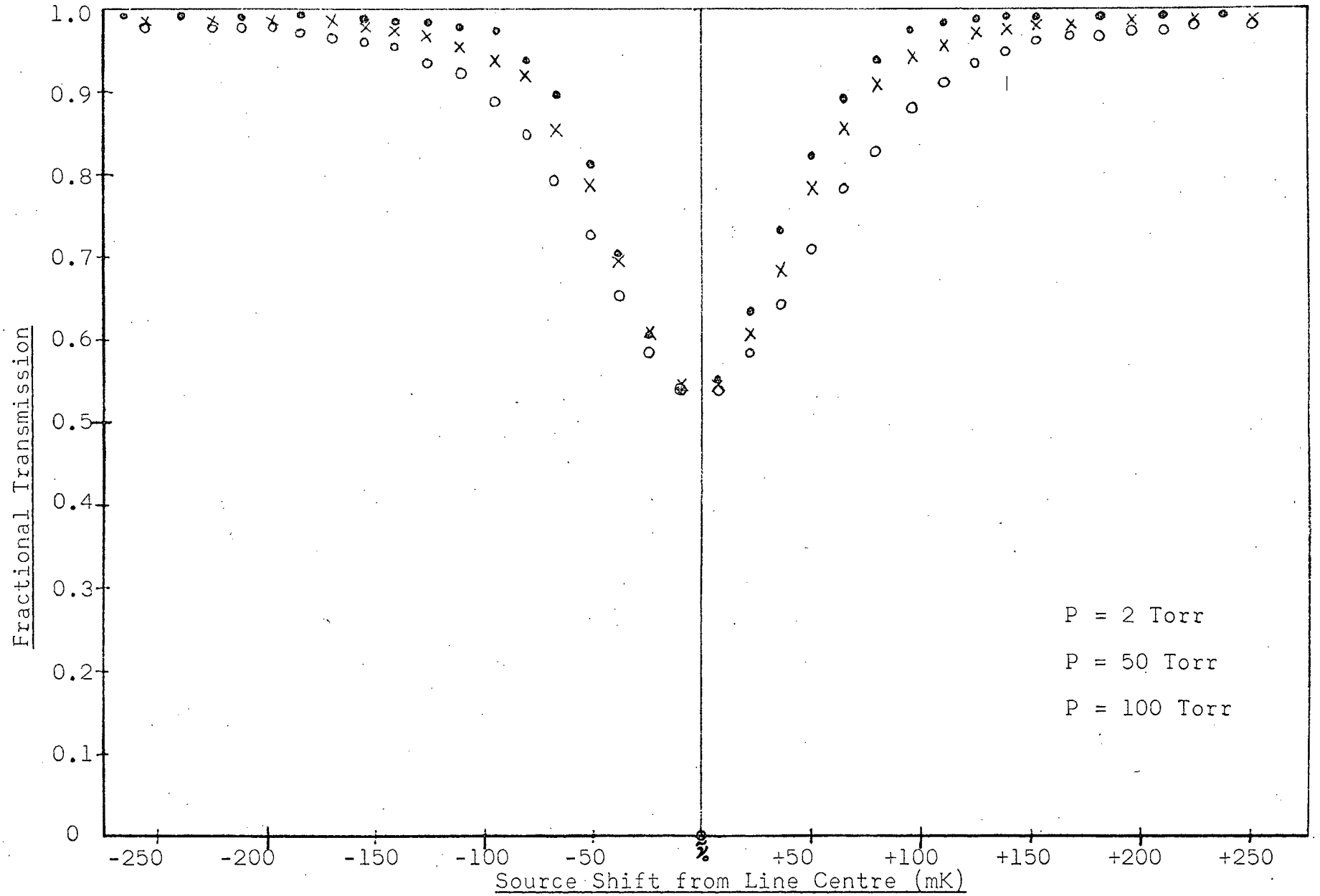

Fig. 7 Transmission Curves for Different Pressures (t_o = 0.53)

B. Detection of Shift

There is a slight but ubiquitous asymmetry of the transmission curves with respect to the designated zero field - zero shift position. However the curves are all more or less symmetric about an ordinate of $\simeq$ + 4 mK. There was no discernable variation of this offset with pressure. As a result it must be concluded that no significant pressure shift has been detected.

Any real shift due to pressure must have been at most less than 4 mK for the 100 Torr absorber. Such minimal pressure shift, in disagreement with the impact theory for a van der Waals interaction, is consistent with the results of Smith (14).

The line centre transmission, t_o, was taken on the axis of symmetry in each case.

C. Line Shape Determination

As a result of the analysis by modelling (as described in Chapter V section B), the parameters of the model of best fit are:

Source	Absorber(s)
$\Delta\nu_{DS}$ = 50 mK	$\Delta\nu_{DA}$ = 48 mK
($\Rightarrow$ T_s = 360 ^{o}K)	($\Rightarrow$ T_a = 325 ^{o}K)
$\Delta\nu_{LS}$ = 6 mK	
(source Voigt A = 0.12)	
K = 1.5	

The Lorentzian half widths of the absorbers, as concluded

from the t_o versus Δt curves (see Figure 10), are tabled below:

Pressure (Torr)	$\Delta\nu_{LA}$ (mK)	Voigt A
2	7	0.14
50	23	0.48
100	48	1.00

The comparison of theoretical and experimental transmission curves for pressures of 2 Torr and 100 Torr are displayed in Figures 8 and 9 respectively. Figure 10 shows the theoretical curves for line centre transmission versus half width for the model of best fit, with the experimental results also displayed. It was primarily from this curve that the assignment of Lorentzian half widths for the higher pressure absorbers was made.

D. Rate of Pressure Broadening - Comparison with Theory

The results tabulated above may most easily be compared with theory by means of a 'rate of pressure broadening' graph - see Figure 11 - in which the absorber Lorentzian half width is plotted against pressure (and density).

The data are insufficient to permit conclusions regarding the linearity of this curve. However, assuming a linear relationship passing through the origin (as predicted by the impact theory) then the best straight line has a slope:

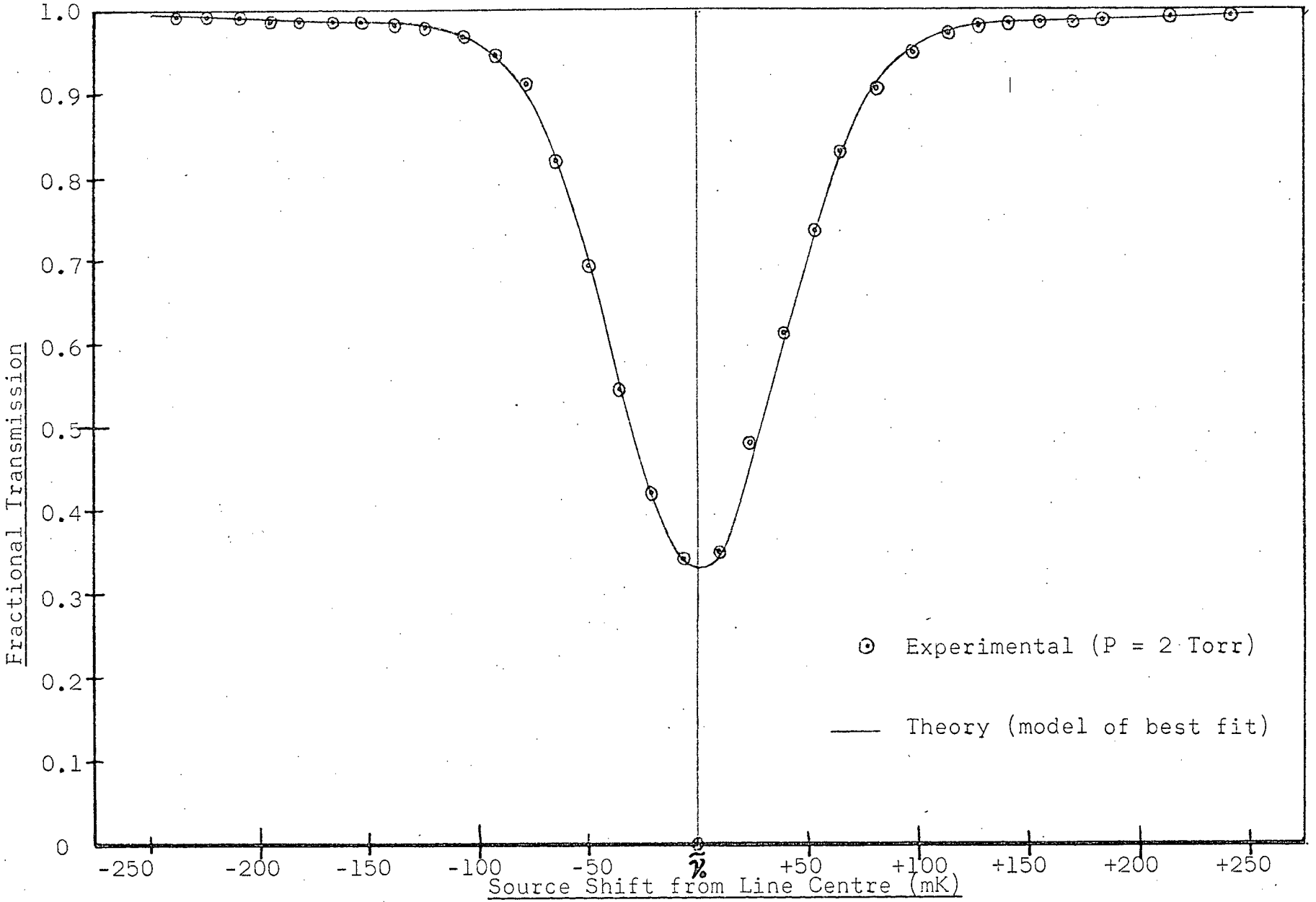

Fig. 8 Transmission Curve: Theory and Experiment (P = 2 Torr)

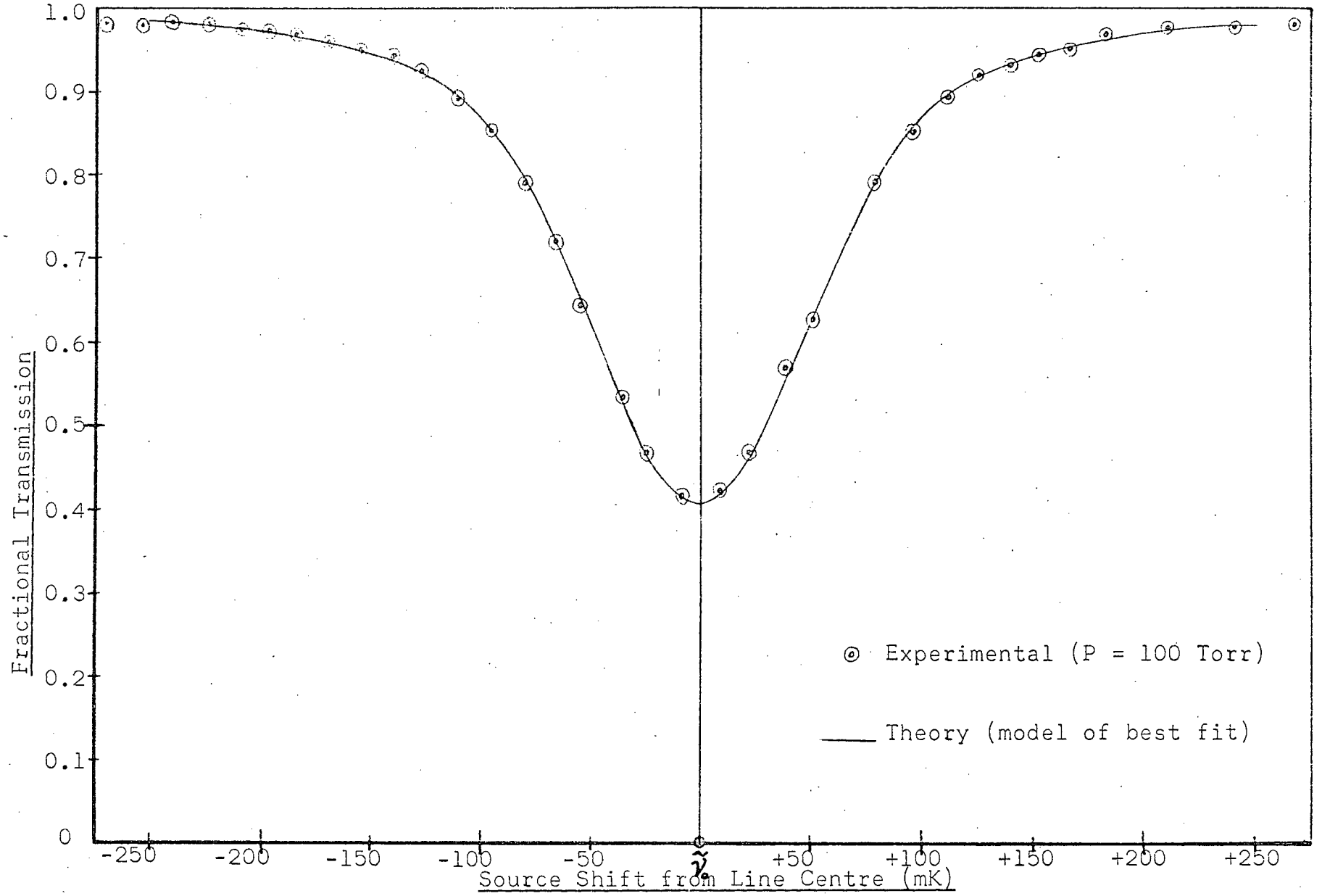

Fig. 9 Transmission Curve: Theory and Experiment (P = 100 Torr)

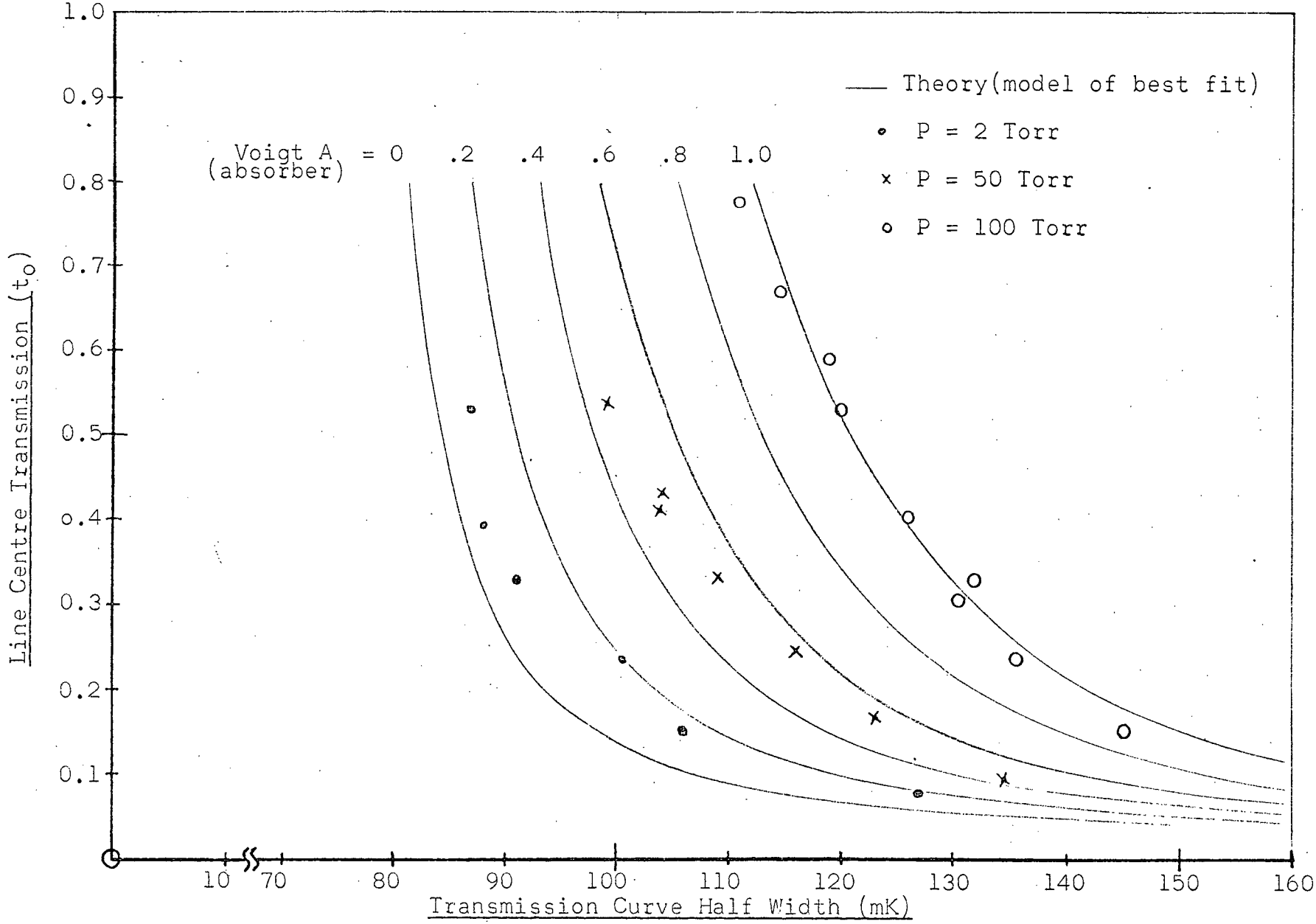

Fig. 10 Transmission Half Width versus Transmission (Theory and Experiment)

$$\frac{\Delta\tilde{\nu}}{n} = 1.6 \cdot 10^{-17} \text{ mK cm}^3$$

Both estimates calculated in the theory (Chapter II, section C) are displayed as well. It can be seen that the experimental results show a rate of pressure broadening nearly 50 % greater than that predicted by theory. However there is close agreement with the semi-empirical rate derived from the results of Smith (14).

E. Validity of Results

(1) Reliability:

Since the results are derived through a complex process of profile analysis and parameter variation, error estimates are difficult and somewhat uncertain. The error estimates shown are primarily based on self-consistency.

In matching experimental and theoretical transmission curves the fitting errors are quite small since the curves are so similar. Variation of the absorber Voigt A parameter by more than $\pm$ 0.05 distorted the shape of the theoretical curve sufficiently to cause rejection of the fit. Similarly, variation of the Doppler half width assigned to the absorber by more than $\pm$ 2 mK altered the width of the theoretical curve enough to make the lack of fit apparent. Moreover variations of these two parameters could not be made altogether independently, for decreases in the assigned Doppler width would eventually necessitate concurrent increases in the assigned Voigt A parameter, etc. As a result the uncertainty

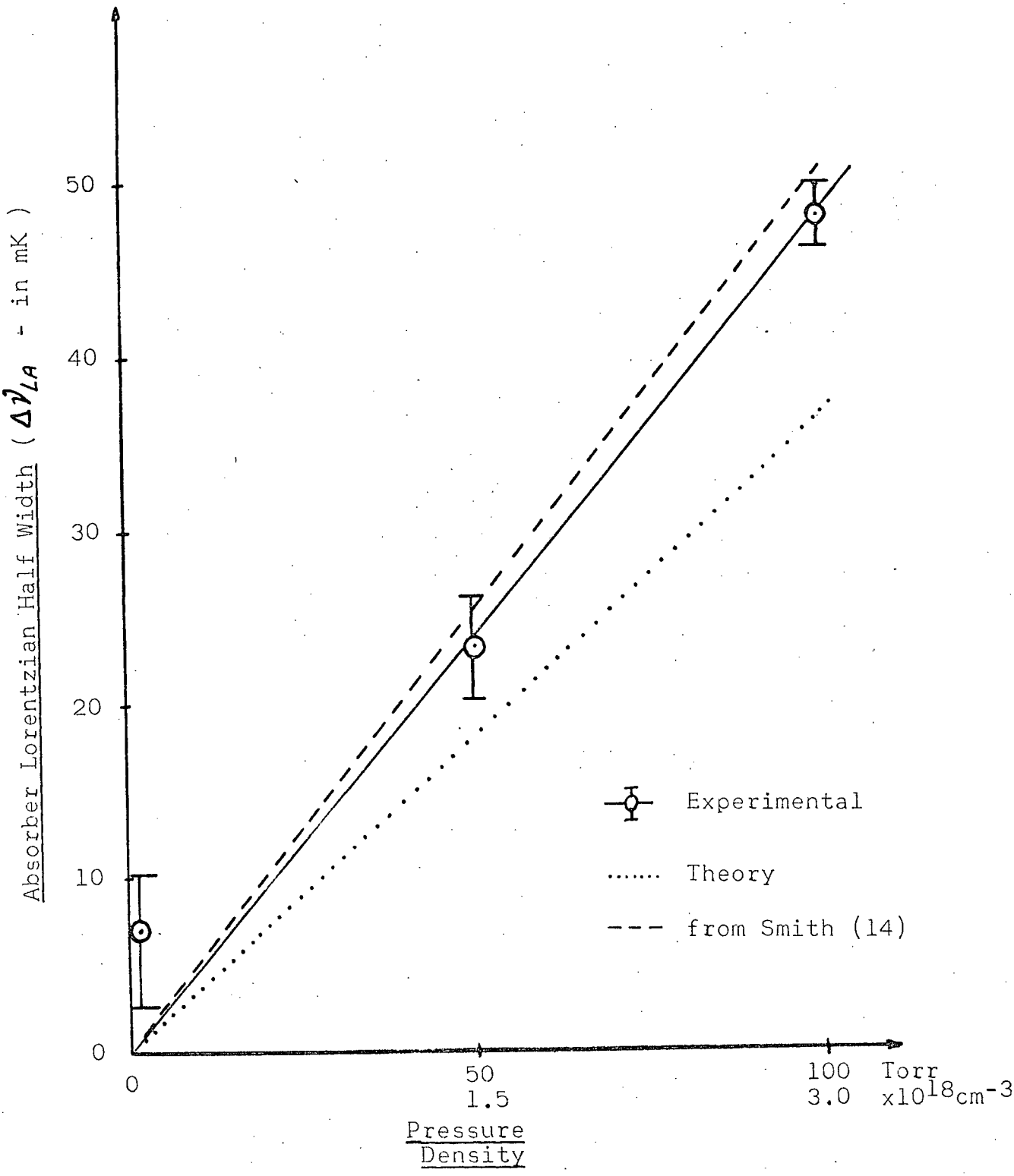

Fig. 11 Rate of Pressure Broadening

in the assigned absorber Lorentzian half width is thereby probably no more than ± 4 mK.

From the transmission versus half width relation (see Figure 10) upon which the final estimates were based there is a range of Voigt A parameters (and hence Lorentzian half widths) spanned by the experimental points.

Pressure (Torr)	$\overline{\Delta\nu_L}$ (mK)	$\Delta\nu_L$ (minimum) (mK)	$\Delta\nu_L$ (maximum) (mK)
2	7	2.5	10.5
50	23	20.5	26.0
100	48	46.0	49.5

These variations, in conjunction with the fitting errors described above, were used as the basis for assigning the confidence limits displayed in Figure 11.

(2) Systematic Errors:

Since all the transmission curves showed the same slight shift of approximately 4 mK, which was moreover independent of pressure, an apparatus error is suspected. This + 4 mK offset is thought to have originated in a failure of the scanning electromagnet to follow perfectly its calibration curve.

This condition results from imperfect regulation of the electromagnet current in the face of variations of the coil resistance due to heating. After the current was reversed (the transition from negative to positive shift) it was to

have been monotonically increased in order to follow the calibration curve. However after each current increment (0.2 amp) the coils warmed further and their resistance increased. There was a tendency for the current to then decrease very slightly, in spite of the regulation provided in the electromagnet current power supply.

This would have taken the magnet off the assumed calibration curve and slightly into the 'interior' of the hysterisis loop. The actual magnetic field would be less than that assumed. This would result in an expansion of the frequency scale for this half of the transmission curve in that the actual field (and Zeeman shift) are less than those assigned. As a result the centre of gravity of the transmission curve would be displaced to the high frequency side (see Figure 12).

In addition to producing the apparent shift, this effect must also have caused apparently wider transmission curves. No attempt, however, was made to correct for this possible error and theoretical profiles were fitted to the centre of symmetry.

The rate of broadening graph (Figure 11) reveals what is possibly the effect of a second source of systematic error. The Lorentzian width assigned to the 2 Torr absorber is apparently too great since all pressure broadening theories predict half widths directly proportional to pressure (and density). In the limit of zero pressure the Lorentzian half width should approach the natural line width (here only $\simeq$ 0.6 mK).

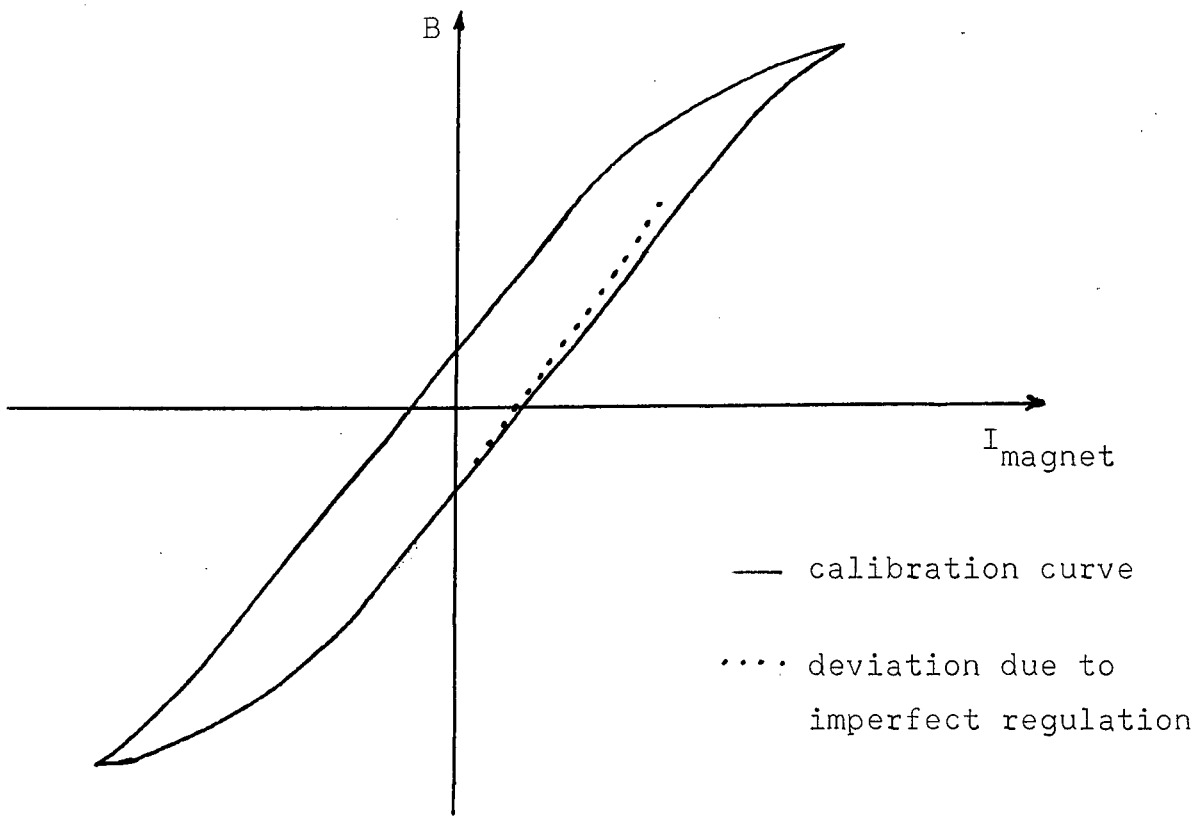

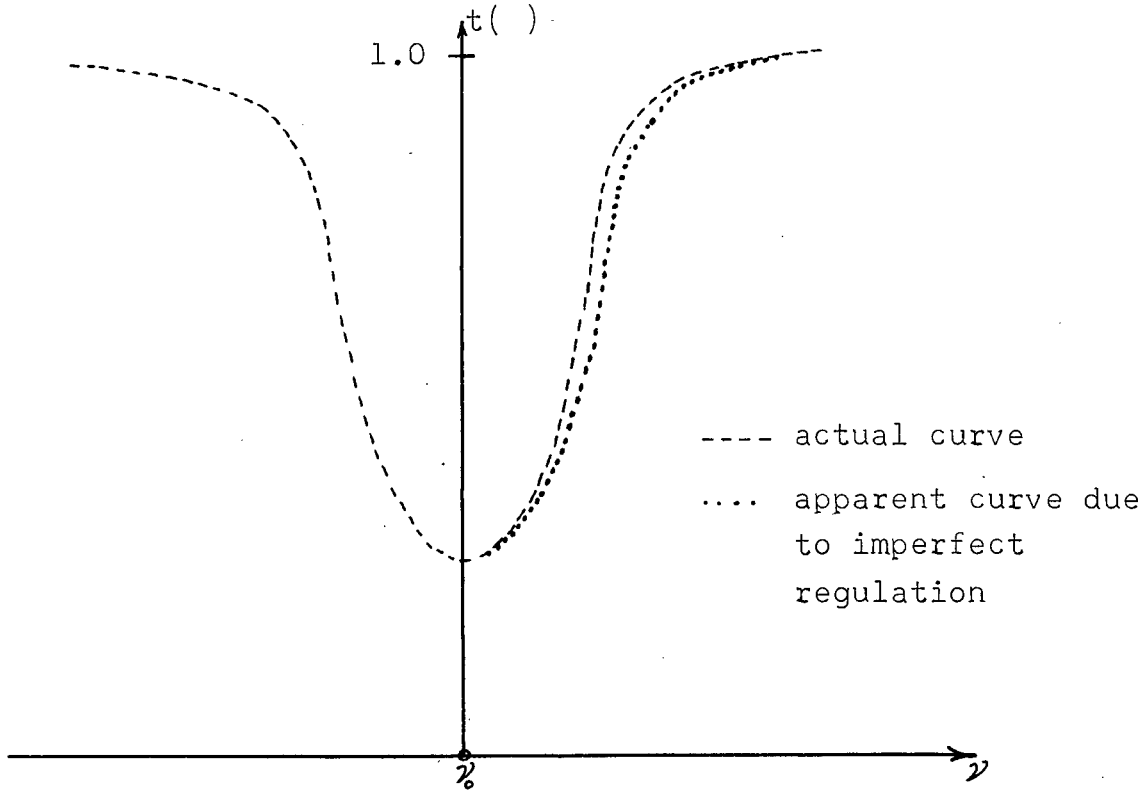

Fig. 12 Effect of Current Regulation Failure

Since this is negligible then for the 2 Torr absorber the expected Lorentzian width should be the van der Waals width of $\simeq$ 1 mK only - outside the confidence limits assigned!

The origin of this apparently excessive Lorentzian width is in all probability unaccounted broadening of the source. Several minor broadening effects which were neglected are:

1. magnetic field inhomogeneities (see Chapter II).
2. alteration of the source line shape as the scanning magnetic field is varied.
3. variations in the self absorption resulting from the inhomogeneous cylinderical nature of the source. (in contrast to the homogeneous, plane-parallel source assumed in the theory)

It has been pointed out by van de Hulst and Reesinck (16) that "the combination of many independent broadening effects tends to yield a Voigtprofile". The source line should thus have had a Voigt type profile, as was assumed. However the Lorentzian component should properly have been greater than the Lorentzian half width ascribed to pressure broadening alone.

In the analysis the source and the 2 Torr absorber were assumed to have had <u>equal</u> Lorentzian half widths since their pressures were equal. Thus an exaggerated Lorentzian half width must have been ascribed to the 2 Torr absorber in order to fit the transmission curves.

Such an error in the source line shape will also create errors in the results for the higher pressure absorbers. However

for these it was found that the Lorentzian widths of the derived line profiles were less affected by changes in the assumed source shape than were those of the 2 Torr absorber. Hence, as might be anticipated from the theory (see equation IVA), the results for the higher pressure absorbers would have been less affected by such an error in the source line shape.

CHAPTER VII

CONCLUDING DISCUSSION

The Zeeman scanning technique has shown itself well suited to the determination of narrow spectral line profiles. The ability to detect differences as low as 5 mK (or 2 mA^{o}) in absorption line width may be considered to represent a resolution of $\frac{\lambda}{\Delta\lambda} \simeq 3 \cdot 10^{6}$, which is difficult to obtain otherwise except with sophisticated spectrographic techniques.

By comparing absorbers at different pressures the extent of pressure broadening for Ne λ6074.3 A^{o} has been determined for glow discharge conditions. It is apparent from the results that even at pressures as low as a few Torr this line will exhibit a non-Gaussian profile. At 10 Torr and 325 ^{o}K the Ne λ6074.3 A^{o} line shows a Voigt A parameter of A = 0.1 (interpolated from Figure 11).

The pressure broadening could be calculated quite well from theory. This is probably true also for other lines of the neon triplet system which are unaffected by resonance effects. Those neon lines affected by resonance broadening likely exhibit Voigt A values even greater than Ne λ6074.3 A^{o} under similar conditions.

Thus the casual assumption of Gaussian profiles for neon glow discharge lines is in error. Where such an assumption is to be made the consequences of the pressure broadening should first be checked.

Close agreement for the rate of pressure broadening has been obtained with values calculated using the impact theory with a van der Waals interaction postulated. The experimental value of $\frac{\Delta\tilde{\nu}}{n} = 1.6 \cdot 10^{-17}$ mK cm^3 agrees with the value derived from the results of Smith (14) to more or less within the assigned confidence limits. The more theoretical value is likewise encouragingly close - to within 50 %. Such good agreement would appear to justify the use of Unsőld's approximation (equation VIII).

The lack of observed shift, consistent with the results of Smith (14), confirms the failure of the van der Waals interaction to properly describe the emitter - perturber interaction in this instance. The inclusion of a repulsive term, as advocated by Hindmarsh, Petford, and Smith (15), is evidently required. Such a consideration falls beyond the scope of the present work and would likely require a more accurate study of the shift.

This is one reason why an investigation of one or two argon lines by this Zeeman scanning technique would be most interesting. Of course argon has also been used in glow discharges for similar experiments (19, 20) to those previously noted (1, 2) so therefore it is desireable to check argon line shapes as well. In addition the results of Smith (14) indicate that argon behaves closely to the predictions of the impact theory with a van der Waals interaction. In particular the shift to width ratio is close

to the 1:2.76 value predicted. Thus for higher pressures such as 50 or 100 Torr the shift should be easily detected. An investigation in argon, then, offers an excellent opportunity not only to check these line shapes but to also further test the Zeeman scanning technique and confirm Smith's findings in the case of argon self-pressure broadening and shift.

For future work several improvements in the Zeeman scanning apparatus can be suggested. The width of the source line is analogous to the apparatus width of a spectrograph or interferometric system in that the source profile is folded with that of the absorber to produce the experimental result. Ideally the source line width should be significantly less than that of the absorber. Then, as suggested by the theory (see equation IVA), the shape of the transmission curve depends almost solely on the absorber's line shape. Such a situation was not achieved in this experiment but where it was approached with the 100 Torr absorber the results are more reliable. At lower pressures the line widths of both source and absorber are primarily determined by Doppler broadening and are thus comparable. Unless drastic cooling or some other means is employed to reduce the Doppler width of the source the ideal narrow - source situation is unrealizable.

Alternately, however, a precise determination of the source line shape will permit an accurate measurement of the absorber line shape. This could be accomplished by reducing the source pressure and optical thickness so that pressure

broadening and self absorption are effectively eliminated. Then Doppler broadening alone would determine the source line shape. These measures would imply also a source of low intensity, reducing the signal - to - noise ratio and very likely necessitating a more efficient detection system than that employed in this experiment. In addition magnetic field inhomogeneity would have to be further reduced to guarantee the absence of any broadening resulting therefrom.

With such improvements the number of "free" parameters to be satisfied in the analysis would be reduced and the results not only more easily obtained but also more reliable.

In view of the encouraging results obtained in this experiment it is hoped that future work, with the apparatus further refined, will be carried out.

BIBLIOGRAPHY

(1) Nodwell, R., van Andel, H., & Robinson, A. : JQSRT 8 , p. 859 (1968).

(2) Seka, W., & Curzon, F.: JQSRT 8 , p. 1147 (1968).

(3) Stansfield, B. : M.A.Sc. Thesis (U.B.C. - 1967).

(4) Bitter, Plotkin, Tichter, Teviotdale, & Young : Phys. Rev. 91 , p. 421 (1953).

(5) Heitler, W. : The Quantum Theory of Radiation ; O.U.P. (3rd Ed. - 1959) Section I, 4(pp. 25 - 34).

(6) Heitler, W. : ibid Section V, 18(pp. 181 - 185).

(7) Nodwel, R., van Andel, H., & Robinson, A. : ibid p. 872.

(8) Ecker, G. & Zöller. O. : Phys. Fl. 7 , p. 1996 (1964).

(9) Griem, H. : Plasma Spectroscopy , McGraw-Hill (1964) Table 4-5.

(10) Irwin, J.C. : Ph.D. Thesis (U.B.C. - 1965).

(11) Foley, H. : Phys. Rev. 69 , p. 616 (1946).

(12) Unsöld, A. : Physik der Sternatmosphären , Springer (2nd Ed. - 1955).

(13) Allen, C.W. : Astrophysical Quantities , Athlone (2nd Ed. - 1963).

(14) Smith, G. : Proc. Roy. Soc. A297 , p. 288 (1967).

(15) Hindmarsh. Petford, & Smith : Proc.Roy.Soc. A297, p.296 (1967).

(16) Van de Hulst & Reesinck : App. J. 106 , p. 121 (1947).

(17) Young, C. : JQSRT 5 , p. 549 (1965).

(18) International Critical Tables V : McGraw-Hill (1929) p.418ff.

(19) Jacobson, T. : Ph.D. Thesis , (U.B.C. - 1969).

(20) Stockmayer, P. : M.Sc. Thesis (U.B.C. - 1969).

APPENDIX I

Flowchart: Computer Calculation of Transmission Curves *(a)

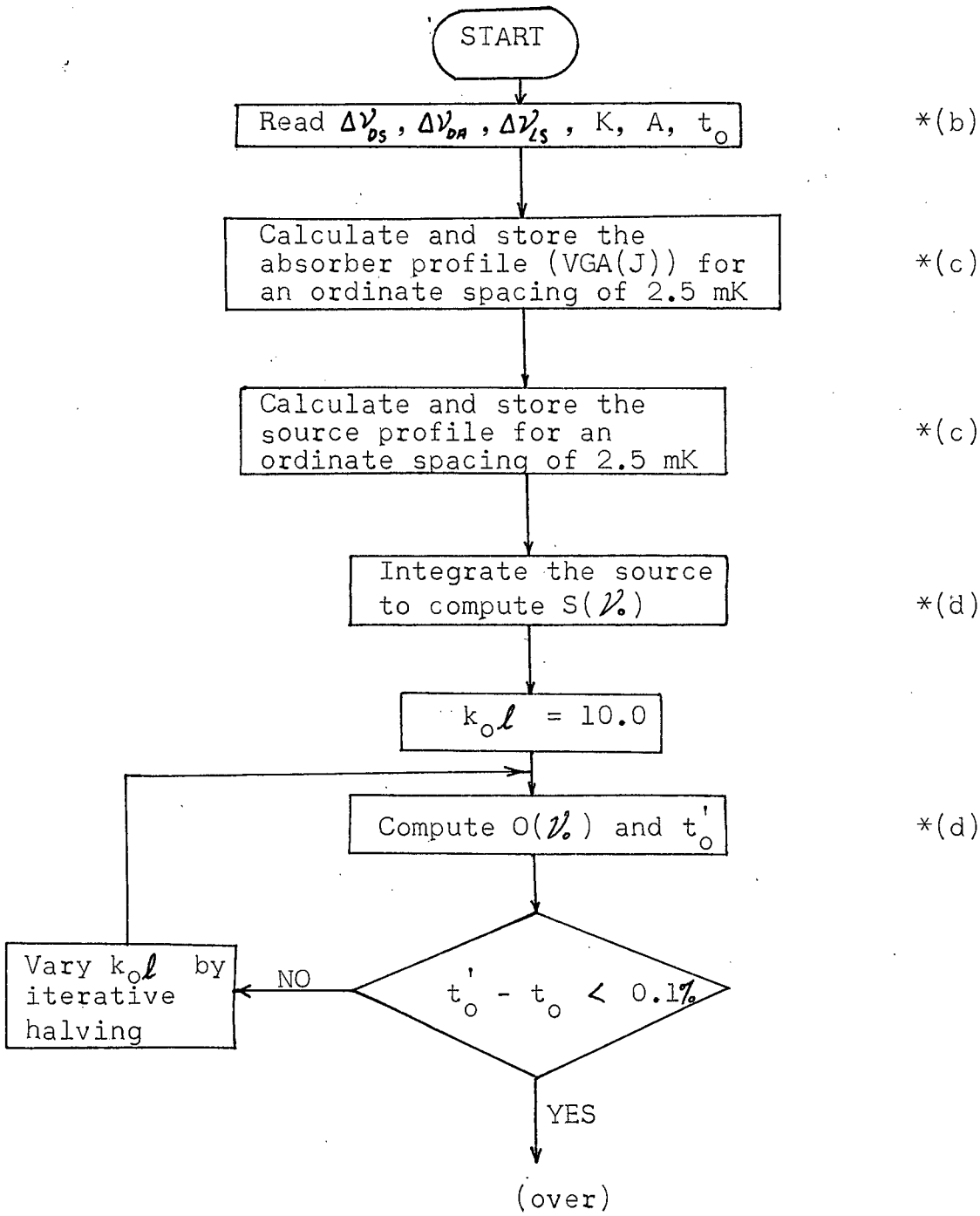

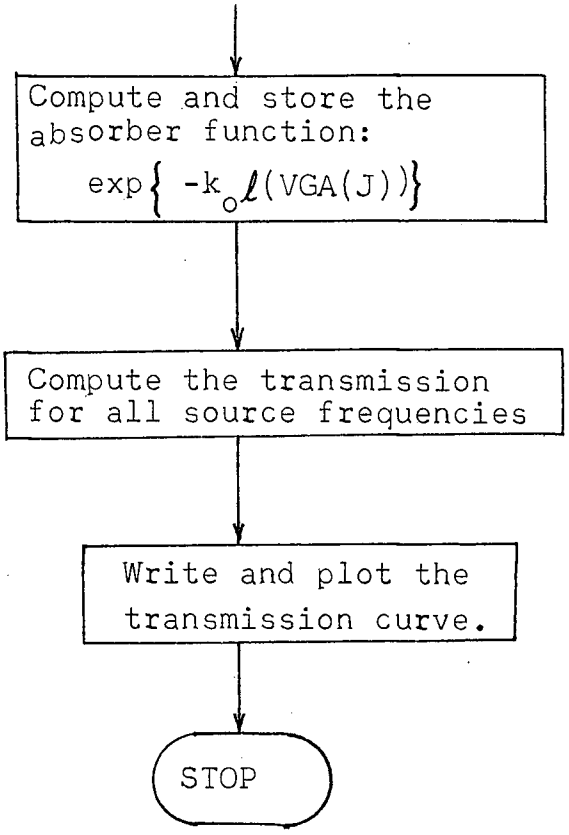

*Notes: (a) The calculations were performed on an IBM 7044 computer.

(b) A is the Voigt A parameter for the absorber; other symbols are as defined in Chapters II and V.

(c) The profile is calculated using the VOIGT subroutine (17) for each specific frequency.

(d) The integration was performed by use of a composite Newton - Cotes formula of order 4 (closed) in 100 steps from - 10 to + 10 half widths.